

**DEVELOPMENT OF A WHEELCHAIR SEAT CUSHION WITH SITE-SPECIFIC
TEMPERATURE CONTROL FOR PRESSURE ULCER PREVENTION**

by

Andrew J. Malkiewicz

Bachelor of Science in Bioengineering, University of Pittsburgh, 2006

Submitted to the Graduate Faculty of
Swanson School of Engineering in partial fulfillment
of the requirements for the degree of
Master of Science in Bioengineering

University of Pittsburgh

2011

UNIVERSITY OF PITTSBURGH
SWANSON SCHOOL OF ENGINEERING

This thesis was presented

by

Andrew J. Malkiewicz

It was defended on

April 5, 2011

and approved by

Michael L. Boninger, MD, Professor and Chair, Physical Medicine and Rehabilitation

Professor, Department of Bioengineering

Professor, Department of Rehabilitation Science and Technology

Patricia Karg, MS, Assistant Professor, Department of Rehabilitation Science and Technology

David M. Brienza, PhD, Professor, Department of Rehabilitation Science and Technology

Professor, Department of Bioengineering

Thesis Advisor

Copyright © by Andrew J. Malkiewicz

2011

DEVELOPMENT OF A WHEELCHAIR SEAT CUSHION WITH SITE-SPECIFIC TEMPERATURE CONTROL FOR PRESSURE ULCER PREVENTION

Andrew J. Malkiewicz, M.S.

University of Pittsburgh, 2011

Pressure ulcers are prevalent and costly, particularly for individuals with impaired mobility and sensation. They are primarily caused by high pressure near bony prominences. Multiple other factors include shear force, friction, temperature, and moisture. Recent research at the University of Pittsburgh was conducted on local cooling effects with respect to skin blood flow. A reduction of skin temperature to 25°C provided a significant benefit to local tissue in healthy controls and subjects with spinal cord injuries. This concurs with prior animal studies which demonstrated reductions in breakdown at lower interface temperatures. Pressure ulcers have been historically managed by providing support surfaces, such as wheelchair seat cushions, to redistribute pressure at the body interface.

Few practical interventions exist to control temperature at this interface; most employ passive cooling methods, which are limited by their inability to modulate applied cooling in response to changes in microenvironment. This study's goal was to develop controlled, local cooling elements for integration into a pressure-redistributing support surface.

A holistic view of temperature control methods in an iterative design process was taken. Features and design specifications were generated using information from the literature. Idea generation and evaluation led to the modification of a multi-cell air cushion capable of controlling temperature in specific high risk areas. Proof of concept experiments were conducted

with respect to interface cooling to a target temperature, redistribution of pressure, and heat and water vapor transmission.

The design delivered local cooling over hour-long trials on able-bodied test subjects. No significant difference in skin temperature ($p>0.16$) was found after 15 minutes of cooling from our target temperature (25°C). The modified cushion showed similar ($p=0.79$) peak pressure index values when compared to the same cushion design without the cooling elements. A thermodynamic rigid cushion loading indenter mimicked the environmental conditions of the body on the prototype for 3-hour duration tests. Significantly lower temperatures were observed after 1 hour of cooling ($p<0.003$). No effect was noted for relative humidity. These experiments successfully demonstrated plausible, integrated cooling elements in a multi-cell air cushion for the delivery of local cooling for pressure ulcer prevention.

TABLE OF CONTENTS

PREFACE.....	XIII
1.0 INTRODUCTION.....	1
1.1 PROBLEM STATEMENT	1
1.2 SPECIFIC AIMS	3
1.2.1 Design flowchart	4
1.3 PRESSURE ULCER BACKGROUND	4
1.3.1 Definition and classification of a pressure ulcer	4
1.3.2 Etiology of Pressure Ulcers.....	6
1.3.2.1 Shear force and friction.....	7
1.3.2.2 Ischemia and Reperfusion Injury	7
1.3.2.3 Moisture and heat accumulation	8
2.0 FORMULATION DESIGN: LITERATURE REVIEW.....	9
2.1 TEMPERATURE EFFECT OF SKIN TOLERANCE TO PRESSURE	9
2.1.1 Animal Studies	9
2.1.2 Human Studies.....	12
2.2 MATERIAL EFFECTS ON CUSHION INTERFACE PROPERTIES.....	14
2.2.1 Pressure	15
2.2.2 Shear force.....	16

2.2.3	Temperature.....	16
2.2.4	Summary	18
2.3	MEDICAL AND COMMERCIAL COOLING EQUIPMENT	19
2.3.1	Rapid hypothermia induction techniques	19
2.3.2	Personal cooling systems	20
2.3.3	Cryosurgical devices.....	21
2.3.4	Summary	22
2.4	DESIGN SPECIFICATIONS	23
3.0	CONCEPT & CONFIGURATION DESIGN	28
3.1	WATER CIRCULATING SYSTEM	28
3.1.1	Analysis of design	31
3.2	DESIGN OF A THERMOELECTRICALLY COOLED AIR CUSHION ...	33
3.2.1	Product layout - Air cushion with thermoelectric elements	33
3.2.1.1	Design layout	33
3.2.1.2	Component summary	35
3.2.1.3	Instrumentation.....	38
3.2.1.4	Air pressure setup procedure.....	40
3.2.1.5	Gel pad and controller configuration.....	40
3.2.1.6	Selection of gel pad materials.....	44
3.2.2	Component refinement - Air cushion with thermoelectric elements	46
3.2.2.1	Increased hydrogel pad size	47
3.2.2.2	Fully enclosed air chamber design	48
3.2.2.3	Revised layout.....	49

4.0	PROTOTYPE EVALUATION METHODS	51
4.1	ADDITIONAL INSTRUMENTATION	51
4.1.1	Thermal imager to measure interface cooling	51
4.1.2	Force sensing array to measure pressure redistribution	52
4.1.3	Thermodynamic rigid cushion loading indenter to measure heat and water vapor transmission.....	53
4.2	EXPERIMENTAL PROTOCOLS.....	55
4.2.1	Verification of interface cooling	55
4.2.2	Verification of pressure redistribution	56
4.2.3	Heat and water vapor transmission	57
4.3	RESULTS	59
4.3.1	Verification of interface cooling	59
4.3.2	Verification of pressure redistribution	61
4.3.3	Heat and water vapor transmission characteristics	63
4.4	DISCUSSION	65
4.4.1	Verification of interface cooling	65
4.4.2	Verification of pressure redistribution	67
4.4.3	Heat and water vapor transmission characteristics	69
4.5	LIMITATIONS	72
4.6	FUTURE DIRECTIONS.....	73
4.7	SUMMARY AND CONCLUSIONS	74
	APPENDIX A	76
	BIBLIOGRAPHY.....	77

LIST OF TABLES

Table 1: Advantages and disadvantages of cooling methods	23
Table 2: House of Quality Matrix.....	24
Table 3: Engineering design specifications	26
Table 4: Example thermal conductivities of gel pad materials relative to copper.....	45
Table 5: Comparison of literature values to HWV test.....	70

LIST OF FIGURES

Figure 1: Steps taken towards the development of a cool cushion.....	4
Figure 2: Diagram of water cooling system. (A) Fan-cooled radiator. (B) Water circulating motor. (C) Flow rate adjustment knob. (D) Foam block cushion with inlaid path for water tubing. (E) In-line water temperature monitor. (F) Power Supply.	29
Figure 3: Thermocouple sensor locations - (A) Thermistor scanning module. (B) Thermistor. (C) Orientation of seated test subject on cooling concept.....	30
Figure 4: Modified tubing layout, reduction in tubing wall and foam thickness.....	31
Figure 5: Example of multi-cell ROHO air cushion.....	33
Figure 6: (Left) - Exploded view of cooling element. (Right) - air cell under load.	34
Figure 7: Potential arrangement of cooling elements within a cushion.....	35
Figure 8: (A) ROHO air chamber. (B) Thermally conductive gel pad. (C) TEC unit. (D) Sensing and control thermistors. (E) Heat sink. (F) Heat sink cooling fan. (G) Support platform and frame.	36
Figure 9: Model and physical layout of cushion design	37
Figure 10: Epoxy sealed border to prevent air loss (yellow) and supporting air chambers (blue)	38
Figure 11: TEC controller board with two power supplies (A)(B) and dual input thermistors (E)(F).....	39

Figure 12: Labview control program GUI	39
Figure 13: Labview control button labels	39
Figure 14: Control thermistor test locations. (A) Within gel. (B) Above gel. (C) Below gel in contact with TEC. (D) On skin of seated user.	41
Figure 15: Plot of interface temperature vs. time for various combinations of control thermistor location and TEC set point temperature. Values averaged over 5 trials, every 500 data points. 20C on top of the gel pad was not tested.	43
Figure 16: Control temperature oscillation about set-point.	44
Figure 17: Gel pad materials - (A) Hydrogel, (B) Polyurethane modified with ceramic beads ...	45
Figure 18: Change in interface temperature from starting temperature (top) and absolute (bottom) interface temperature of gel pad materials.....	46
Figure 19: Comparison of first (A) and second (B) generation hydrogel pads.	48
Figure 20: Underside view of gel pad secured in ROHO air chamber.	49
Figure 21: Quickie wheelchair with and without modified ROHO cushion.	50
Figure 22: Underside of machined drop seat illustrating mounted heat sink and cooling fan.....	50
Figure 23: FSA pressure mat system.	53
Figure 24: TRCLI components	54
Figure 25: Labview controller for Fieldpoint data loggers.....	55
Figure 26: Modified ROHO and wheelchair base beneath TRCLI	59
Figure 27: TRCLI resting on calibrated ROHO cushion.....	59
Figure 28: Average values at each time point with respective CI.	60

Figure 29: (A) Example thermal images (°C) before (left) and after (right) cooling trials. Dashed outline represents same area before and after cooling. (B) Thermal image orientation. 61

Figure 30: Example of pressure mat data. Location of cooler labeled in red over left IT region. 62

Figure 31: Plot of PPI for cushion comparison..... 62

Figure 32: Average values for contralateral sides of cool cushion. 64

Figure 33: All trials for HWV characterization tests. 64

Figure 34: Examples of pressure mat readings. (left) bottoming out - (right) air loss 69

PREFACE

First, I would like to thank my parents and siblings for their tireless support and love throughout my graduate studies. I would like to thank my thesis advisor, Dr. David Brienza, and my thesis committee, Ms. Patricia Karg and Dr. Michael Boninger for their expertise, feedback, and guidance. I thank Yi-Ting Tzen and Ana Allegretti for their technical and moral support. Both of you assured me there was a light at the end of the tunnel, both personally and professionally. I also thank Sue Fuhrman for her mentorship, friendship, and guidance. I thank Erik Porach and David Smeresky for their assistance with testing, design, and fabrication. For Davey in particular, thank you for being a wonderful undergraduate assistant. I wish you great success in your future. To everyone at Bakery Square: Debby, Cheryl, Joe, Linda S, Linda V, Rich, Mary Jo, Chaz, Hassan, Shilpa, Shaley, and Emily, thank you for your friendship, support, and feedback over the last two years. I also thank my Pittsburgh family of James Kurasch, Mary Kurasch, and Denis Cunningham for all our wonderful memories and for believing in me from the start. Finally, I would like to thank the National Institute on Disability and Rehabilitation Research (NIDRR), Rehabilitation Engineering Research Center (RERC) on Spinal Cord Injury, and the University of Pittsburgh for their financial support.

1.0 INTRODUCTION

1.1 PROBLEM STATEMENT

Pressure ulcers afflict 1.3 to 3 million patients per year [1, 2] representing 3% to 29.5% of acute and long term care facility patients in the US and internationally [3-7]. Patient groups at risk for PU in healthcare settings include the elderly, persons with impaired mobility (such as spinal cord injuries, or head trauma), persons with poor nutrition, and those with more severe comorbidities such as diabetes or stroke [8-11]. People with these conditions are generally unable or unaware to weight shift during prolonged pressures associated with sitting or lying down. In 2006 the Agency for Healthcare Research and Quality published data collected from a sample of national inpatient centers which highlighted a frequency increase of 280,000 to 450,000 (63%) in hospital acquired pressure ulcers from 1993 to 2003 [10]. These data serve to warn us that despite advances in wound care protocols, support surfaces, and medical technologies, current practice guidelines for pressure ulcer prevention need to be improved upon. Today pressure ulcers remain very costly in terms of recovery time, reduction in quality of life, and finances; *prevention* of pressure ulcers is more important than ever.

Prolonged exposure to pressure has long been attributed as the primary factor in pressure ulcer development [12, 13]. Pressure is defined as “force per unit area exerted perpendicular to the plane of interest” [14]. Early research suggested that localized pressure resulted in tissue

ischemia, or reduction of blood supply, which in turn limits exchange of nutrients, metabolites, and waste products through capillaries and larger blood vessels [12, 13, 15]. Underlying tissue necrosis results in ulceration of the skin [16-18]. However, there are other risk factors associated with pressure ulcer development at the local level. Cofactors such as shear, friction, interface temperature, and moisture all contribute to the skin breakdown historically assumed to be caused by external pressure alone [9, 19].

Recently, our laboratory has conducted research on local cooling with respect to skin blood flow. The “results showed that both fast and slow cooling provided a protective effect on ischemic tissue by decreasing the metabolic demand and suppressing the smooth muscle activity [20, 21].” These findings concurred with prior animal studies that demonstrated similar decreases in tissue susceptibility to damage at lower skin temperatures [22-24]. Pressure reducing support surfaces, such as wheelchair seat cushions, have been shown to be effective in decreasing risk for pressure ulcer development in a variety of settings [25-27]. A support surface is defined as any “specialized device for pressure redistribution designed for management of tissue loads, micro-climate, and/or other therapeutic functions (i.e. any mattresses, integrated bed systems, mattress replacements, overlay, seat cushion, or seat cushion overlay)” [14]. Currently, very few options exist to manage temperature at the support surface interface; of those that exist, almost all utilize some form of passive cooling or open-loop control mechanisms. Passively cooled support surfaces are limited by their steady state temperature and thus may not be sufficient for all user environments and needs. Open-loop systems do not respond to changes in demand as skin temperature rises and falls. By combining a pressure-reducing support surface and controlled, localized cooling, a medical intervention could be developed to better protect the skin of individuals at the highest risk for pressure ulcer development.

1.2 SPECIFIC AIMS

The purpose of this study is to generate local cooling elements which can be integrated to improve wheelchair seat cushion design for tissue integrity management. This cushion will be distinguished from currently existing cooled support surfaces in two critical ways. First, a closed-loop control system will allow the cushion to modulate its cooling output in response to changes in cushion interface temperature; this will be accomplished by imbedding feedback mechanisms in the cushion to maintain a therapeutic temperature. Second, this cushion will provide cooling to select areas most at risk for tissue breakdown (e.g., ischial tuberosities); in this way core normothermia is maintained while local cooling takes place where protection is needed the most.

Specific Aim 1 - Develop design specifications for temperature control cushion

Specific Aim 2 – Conceptualize cooling elements, develop & fabricate prototype

Specific Aim 3 – Develop methodologies to evaluate temperature control features of prototype with respect to:

- Verification of target temperature delivery (25°C)
- Ensuring cushion modifications do not adversely affect pressure redistribution characteristics
- Heat and water vapor transmission

1.2.1 Design flowchart

Figure 1 details steps carried out to better organize and report the process used to formulate our design goals, proof of concept tests, part configuration, and final prototype evaluation. This engineering design layout was summarized from Eggert's [28] guidelines and loosely outlines the contents of this report. In this manner the idea generation, conceptualization and feasibility studies, individual part layouts, and prototype testing methods are detailed below:

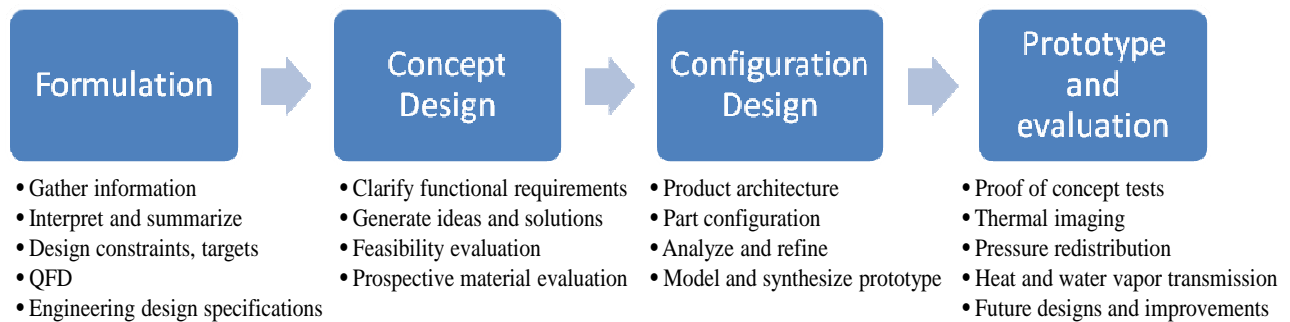


Figure 1: Steps taken towards the development of a cool cushion

1.3 PRESSURE ULCER BACKGROUND

1.3.1 Definition and classification of a pressure ulcer

The National Pressure Ulcer Advisory Panel defines a pressure ulcer (PU) as a localized injury to the skin and/or underlying tissue usually over a bony prominence, resulting from a complex combination of localized pressure and other risk factors [29]. The Centers for Medicare and

Medicaid Services (CMS) reported that almost 10% of nursing home residents and up to 40% of all patients with spinal cord injury acquired at least one stage of a pressure ulcer in their lifetime, a majority of which resulted in significant medical interventions or hospital stays [30, 31]. A pressure ulcer can lead to amputation, sepsis, or death if left untreated or unrecognized. A study analyzing mortality rates adjusted for comorbidities and age reported 114,380 pressure ulcers as a contributing cause of death identified from national multiple cause of death data in 2001 [32]. Roughly 19% of these deaths reported the pressure ulcer as the underlying cause [33].

Retrospective studies estimate the price of managing a high stage pressure ulcer from \$70,000 to \$200,000 in direct hospital costs and annual expenditures could tower over \$11 billion per year in the US alone [2, 34, 35]. Nine out of every ten hospitalizations related to pressure ulcers were covered by government health programs; roughly 66% by Medicare and 23% by state Medicaid [10]. Sixty-seven percent of pressure ulcers are found on the buttock and hip, specifically on the sacrum, ischial tuberosities, and greater trochanters [11]. Other locations have varying degrees of soft tissue between them and bony prominences, including elbow, heel, ankle, occipital, ear, and patella [11, 36]. Pressure ulcers can be classified in severity by various ‘stages’. Stage I pressure ulcers are classified as “Intact skin with non-blanchable redness of a localized area usually over a bony prominence. Darkly pigmented skin may not have visible blanching; its color may differ from the surrounding area.” The most severe stage IV ulcers are defined as “Full thickness tissue loss with exposed bone, tendon or muscle. Slough or eschar may be present on some parts of the wound bed. Often includes undermining and tunneling” [29]. To emphasize the importance of prevention for clinically acquired pressure ulcers, the Centers for Medicare and Medicaid Services no longer issue reimbursement to healthcare

facilities for stage III and IV pressure ulcers that are not documented on admission as of October 1, 2008 [37].

1.3.2 Etiology of Pressure Ulcers

Prolonged exposure to pressure over a bony prominence has been routinely demonstrated as the primary etiological factor for developing a pressure ulcer [19, 38, 39] . Evidence has yet to demonstrate whether these injuries occur initially at the skin surface, within deeper tissue such as muscle, or from a non-specific interaction of both [16]. Landis suspected that localized pressure occluded capillaries and experimentally derived the value of 32 mmHg as a capillary closing pressure [40]. These findings were further investigated by Kosiak in one of the earliest animal studies on the effects of constant and alternating pressures on rat hamstring and surrounding skin [12]. By comparing the histology of healthy controls to a spinal cord injury experimental group where innervation to the hamstring area was severed, he noted the changes to both skin and deep tissue. No damage was observed at 35 mmHg over any time course; muscle tissue was highly susceptible to pressures as low as 70 mmHg at only two hours of exposure. There was little difference between the healthy and paraplegic rat groups, which suggested that innervation is not a direct cofactor in PU development. Studies following this early work suggested an inverse relationship between length and magnitude of local pressure and its effect on pressure ulcer development [18, 41, 42]; *as applied pressure increases in both length and magnitude, the skin's tolerance to breakdown decreases in duration*. Intrinsic risk factors include age, nutritional status, disease comorbidities (diabetes, spinal cord injury, muscular dystrophy) leading to reduced mobility, and incontinence [43]. Extrinsic factors aside from pressure include local friction, shear force, moisture, and heat accumulation [19]. Healthcare professionals use a

variety of tools to characterize an individual's risk for developing a pressure ulcer in clinical settings. Scales, such as the Braden Scale, seek to capture patient information with respect to these aforementioned intrinsic and extrinsic risk factors [44].

1.3.2.1 Shear force and friction

Pressure induces direct mechanical deformation of skin and underlying tissue. Shear force or “sliding force” is applied to the surface through pressure gradients acting perpendicular to the direction of applied pressure [45]. Goldstein and Sanders [46] demonstrated a relationship similar to Reswick and Rogers’[41] summation of the pressure-time inverse relationship: as shear force applied to tissue increases, tissue tolerance decreases. Friction is defined as the “resistance to motion in a parallel direction relative to the common boundary of two surfaces”[14] and has been shown to decrease overall tissue tolerance to prolonged pressure and shear [47, 48].

1.3.2.2 Ischemia and Reperfusion Injury

Prolonged pressure exposure subjects local tissue to ischemia, defined as localized reduction in blood and/or lymphatic circulation [49]. On a cellular level, metabolic activity and exchange are severely reduced by ischemia [13, 47]. When local pressure is relieved, there is a natural brief increase in blood flow known as reactive hyperemia to compensate for the buildup of metabolic wastes and oxygen deprivation [21]. This influx of oxygen rich blood can cause ischemia-reperfusion (IR) injury as toxic levels oxygen-derived free radicals overcome the area's natural compensation ability [15]. IR injury occurs in many organ systems [50] and is a major factor in the development of pressure ulcers; this previously underestimated phenomenon helps explain why some patients develop PU despite receiving standard of care pressure management.

1.3.2.3 Moisture and heat accumulation

While the presence of elevated tissue temperatures has been linked to pressure ulcer formation, the exact mechanism of impact remains unexplained. Elevated or decreased temperature is linked to the rate at which essential reactions take place [51], including but not limited to mass transport, metabolism, exchange of nutrients and waste products, and infiltration of cytokines [15, 50-53]. Other factors include inhibition of temperature-mediated capillary mechanisms, changes in blood viscosity, and increases in tissue stiffness [54]. Tissue exposed to the highest pressures on support surfaces (IT, sacrum, trochanter) are at the highest risks when coupled with ischemic events and resultant reperfusion injury when pressure is relieved. The metabolic demand from increased temperatures exposes tissue to a substantially higher risk of PU formation [55]. Moreover, local temperature increases result in perspiration increases and moisture buildup; this moisture macerates the skin lowering its pressure tolerance [56, 57]. The combination of temperature and humidity (moisture) effects with respect to a support surface is known as the local microenvironment [58].

2.0 FORMULATION DESIGN: LITERATURE REVIEW

2.1 TEMPERATURE EFFECT OF SKIN TOLERANCE TO PRESSURE

As previously mentioned, the objective of this study was to generate design specifications and features that can be used to manage interface temperature of a pressure redistributing cushion. Literature studies on skin cooling, technologies used to measure and quantify tissue temperature, and how existing support surfaces responded or accommodated changes in temperature were selected and examined. The following investigations in both animal and human models sought to better understand the effects of temperature on PU etiology, as well as to develop tools and support surface technologies to analyze and alleviate elevated interface temperatures in both experimental and clinical settings.

2.1.1 Animal Studies

Kokate et al. were responsible for one of the first animal models demonstrating tissue tolerance by varying duration and value of applied pressure over four skin temperatures [59]. An experimental apparatus reliably and repeatedly applied a metal indenter disc to the dorsal aspects of swine at 100mmHg over five-hour periods. The discs were outfitted with heating elements and water cooling channels to generate temperatures above or below core body temperature, respectively. Temperatures of 25, 35, 40, and 45°C were simultaneously applied alongside the

contact pressure. The animals were then monitored during a four-week follow up and recovery period; measurements of edema, local tissue perfusion, and skin surface temperature were performed by blinded observers and tissue samples were taken seven days post-pressure/temperature application for histological analysis. Visually observed surface changes over the twenty-eight day follow up period were compared alongside the histological analysis summarized above to assess the effect of temperature and pressure on overall skin health. Applied temperature of 45°C resulted in partial to full epidermal necrosis, observable damage of subdermal structures, and severe muscle damage. Applied temperature of 40°C was less severe than the highest temperature state but showed only moderate muscle damage. Unfavorable results at 35°C varied individually between experimental subjects, and were generally isolated to areas directly above bony prominences, with little to no epidermal or dermal damage. In general, higher temperatures correlated with increases in tissue damage. Moderate to severe tissue damage were additionally observed at *all* temperatures above 25°C. This suggested that lower skin temperatures could exhibit a protective effect that would allow tissue under bony prominences to sustain higher pressures for longer periods of time.

Iaizzo [60] conducted a follow-up study using this previously established methodology to further refine the “threshold temperature below which focused cooling would minimize the potential for wound formation.” In this study there were two sets of experiments conducted on the dorsal skin of swine. The first was a constantly applied pressure of 100mmHg for 2, 5, or 10 hour periods, paired with the same temperature range as the pilot study (25, 35, 40, 45°C). In the second set, 100mmHg was applied for 10 hour intervals at temperatures of 25, 27.5, 30, and 32.5°C. Again, histology analysis verified marked increases in tissue damage for higher temperatures and duration, whereas minimal damage was seen at all pressure durations for low

skin temperature trials. In fact, these results were true at any focal cooling temperature $< 30^{\circ}\text{C}$, with the most beneficial outcomes at the lowest applied temperatures. Also to note, deep tissue and muscle demonstrated greater sensitivity at the higher applicator temperatures than compared to the epidermis, dermis, and subcutaneous fat layers. This data is consistent with previous studies focused primarily on pressure which concluded pressure ulcers originate in deep tissue and work upwards [61].

Patel et al. worked to better understand the local tissue response of increased or decreased temperature with respect to pressure, skin blood flow (perfusion), and stiffness [54]. Three sets of experiments detailed combinations of temperatures and applied pressures which activated/inhibited auto-regulatory mechanisms of blood flow in the skin of fuzzy rats. In order to demonstrate the effect of skin perfusion in unloaded tissue, the first set of experiments applied a low-constant pressure of 3.7 mmHg to the skin at 28°C , 30°C , 32°C , 34°C , and 36°C . Skin perfusion increased with each temperature increment, which suggested normal vasodilation occurred at even markedly increased skin temperatures for low pressure levels. The second set of experiments applied incremental pressures from 3.7 to 62mmHg under 28 and 36°C . They observed the same increases in perfusion seen in the first experiment at higher temperatures, although these increases tapered off at any pressure > 25 mmHg for both 28 and 36°C . The authors explained that the normal vasodilatory mechanisms were unable to compensate for the mechanical loading of these higher pressures. In a third experiment, tissue displacement via LVDT (linear variable differential transformer) was studied in response to combinations of pressure and temperature as conducted above to calculate changes in stiffness with respect to pressure and temperature. Higher temperatures resulted in stiffer tissue, with markedly less creep than without heating at all levels of pressure. Decreased ability to maintain proper blood

flow and stiffer supporting tissues which poorly dissipate load both could contribute towards the formation of pressure ulcers.

Lachenbruch took a retrospective look at published laser Doppler and tissue oxygenation data from several of the aforementioned studies in order to quantify this protective effect provided by local cooling [62]. Using graphical techniques, he extrapolated that a pressure drop from 56mmHg to 40mmHg is equivalent to an 8°C drop in skin temperature; nearly a 30% reduction in applied pressure. He then equated this protective effect to the pressure reduction granted from high end support surfaces and infers that an inexpensive support surface capable of providing 5°C of cooling relative to normothermal interface temperatures would have the equivalent pressure reduction of surfaces costing nearly double.

2.1.2 Human Studies

The effects of local cooling on skin tolerance to pressure have not been completely explained in the literature, although several methods of direct and indirect measurement of cooling effects have been developed. In 1989 Meijer et. al developed an indirect method of calculating relative ischemia in an area of pressure application [63]. A relatively high pressure (375 mmHg) was applied to the trochanter region of elderly nursing home residents. Skin temperatures were recorded by thermocouples affixed to the skin at the site of application. A nearby control measurement was also taken for comparison. A skin temperature decrease took place during the period of pressure application, although these values were not reported. This temperature decrease was expected because the heat transported by blood flow is much greater than that generated by local metabolism [64, 65], and so restriction of blood flow should naturally result in a decrease in temperature. When the pressure was relieved from the application site, normal

blood flow resumed after a brief latency period and the surrounding area gradually warmed. Pressure ulcer susceptibility was calculated by summing the recovery time and the time constant of the re-warming period. The measure was sensitive enough to distinguish between at-risk elderly patients (those with a documented history of previous pressure ulcers or multiple risk factors as described above) and healthy young controls in terms of susceptibility. No statistical difference was found between the young healthy control group and non-risk elderly population (those with no history of PU or comorbidities). No pressure ulcers resulted from the application of the measurement apparatus. The value of this study is that it sought to measure pressure ulcer risk through an indirect means. Future experimental tools derived from local temperature measurement and skin blood flow response following pressure application allowed researchers to perform analyses on humans without biopsy and histology.

In 2002 Meijer teamed with van Marum et al. to reinvestigate the susceptibility to pressure ulcers as the result of a local stimulus [66]. Instead of an applied pressure, local cooling was used to initiate vasoconstriction and generate a similar temperature-time response as described above. Their hypothesis was that pressure ulcer incidence could be predicted by the velocity of the local blood flow response after cold application (17°C). Patients who did not develop pressure ulcers during the follow-up period had significantly shorter recovery time constants than those who had future skin breakdown, although the difference between initial and final temperature was nonsignificant.

A study conducted at our laboratory illustrated the protective benefit of lower skin temperatures at various cooling rates coupled with pressure [20, 21]. As previously mentioned, people with spinal cord injury are at a high risk of developing pressure ulcers and generally have impaired thermoregulation following their injury [67, 68]. The effect of cooling was assessed

using a noninvasive measure of the reactive hyperemic response in both healthy controls and participants with various levels of spinal cord injury. Participants were subjected to three test sessions: 60mmHg pressure alone, pressure with cooling applied at a slow rate ($-0.033^{\circ}\text{C}/\text{min}$), and pressure cooling applied at a fast rate ($-4^{\circ}\text{C}/\text{min}$). The skin temperature was lowered to 25°C at the point of pressure application. The magnitude of the reactive hyperemia in each subject was a direct measure of the severity of the local tissue ischemia. For healthy controls, reactive hyperemic responses was reduced by both fast and slow cooling rates, and for all subjects metabolic demand was shown to increase only when local cooling was absent. This suggests that local skin cooling presents a beneficial effect to ischemic tissue in participants with or without SCI and may increase tissue tolerance to pressure during weight bearing scenarios. Based on the aforementioned human and animal studies, targeting a skin temperature of **approximately 25°C would maximize the protective potential of our cool cushion design.**

2.2 MATERIAL EFFECTS ON CUSHION INTERFACE PROPERTIES

Design specifications for a cooled cushion were generated by looking at the literature regarding composition and performance of currently existing cushions with respect to pressure redistribution and microenvironment. Standardized reviews and observational studies of cushions arranged by composition and features were examined. Foam, viscoelastic foam, and fluid filled (air/water/liquid) cushions were chosen for evaluation because of their high representation in the literature and potential ease of modification [19]. Foam is defined as a “lightweight cellular material resulting from the introduction of gas bubbles into a reacting polymer” [69]. Foam can be classified as open cell, where gases and liquids can pass through the

foam in a porous manner, or closed cell, in which the foam is non-permeable [14]. Viscofoams or “memory foams” consist of “flexible matrix material that has both elastic (displacement-dependent) and viscous (time-dependent) properties” [69]. This classification also includes pure gel cushions [19]. As the name suggests, fluid-filled cushions are generally composed of viscoelastic, aqueous, or air filled chambers. These chambers exhibit passive movement of fluid from one area to another in response to distributions of seated pressure [19]. By evaluating cushions grouped by construction material, decisions could be made as to what features would bring our cushion design closest to ideal performance.

2.2.1 Pressure

While the overall goal was to identify solutions for controlling cushion microclimate, the ability to appropriately redistribute interface pressure is still a primary concern for the design. Support surfaces aim to reduce interface pressure by two main processes: immersion and envelopment [19]. Immersion is the “depth of penetration (sinking) into a support surface” [14]. High pressures concentrated at bony prominences can be spread over neighboring areas as they immerse into the support surface. Envelopment is “the ability of a support surface to conform, so to fit or mold around irregularities in the body” [14]. Taken together these two measures illustrate how well a particular support surface redistributes load and minimizes interface pressure.

Foam deforms in proportion to its applied load and is a relatively stiff material choice, mainly due to the increased thickness required to adequately support pressure loads [19]. Over time and extended use, mattresses and cushions can bottom out due to structural wearing of the natural air space within its composition [19]. An advantage to foam cushions is their ability to be

modified into contours, segments, or cut-outs in order to accommodate a wide range of seat cushion users [70]. Air cushions have good immersion and mid-level envelopment, if properly inflated to the appropriate internal air pressure. Under and over-inflation can cause bottoming out and pressure increases, although normal operation exhibit satisfactory pressure redistribution[19]. Viscous fluid filled cushions also perform well with pressure unless the material moves out from under bony prominences [71].

2.2.2 Shear force

Forces generally coupled to the application of pressure are shear forces, defined as “the force per unit area exerted parallel to the plane of interest.” These forces generate distortive shear strains as detailed in section 1.3.2.1. Early studies comparing support surfaces with respect to shear force demonstrated better performance of gel or air cushions than standard foam material types [72, 73]. A previous study conducted in our laboratory evaluated cushions in terms of interface shear characteristics [74], utilizing a shear force sensor and standardized horizontal displacement test. The lowest shear stresses were observed in viscous fluid cushions, followed by air, and then elastic and viscoelastic foams at 10, 15, and 20 mm of horizontal displacement.

2.2.3 Temperature

The temperature response of cushion composition materials was given a high amount of focus since lower interface temperature before modifications would most likely give rise to improved outcomes after incorporating methods for closed loop cooling. Early human studies

investigating skin temperature focused around the interaction between a given support surface, time, and the resulting skin temperature, as these surfaces directly impact the microclimate effecting tissues at risk for pressure ulcers [58]. Fisher and Kosiak et al. recorded skin temperatures under ischial tuberosities and posterior thighs during 30 minute test periods on several commonly prescribed seat cushions [55]. They noted increases of temperature under the IT on standard foam cushions; whereas cushions composed of materials with higher specific heats (water floatation and gels) demonstrated decreases or non-significant increases in temperature. This can most likely be attributed to the testing duration being insufficient to achieve a thermal steady state for these cushions. Stewart and Cochran et al. conducted yet another investigation of support surface heat distribution capability, in which they measured skin temperature and relative humidity for commercially available cushions (foam, viscoelastic foam, gel, water floatation, and air) [75]. Temperature, heat flux, and relative humidity data were collected by affixing appropriate sensors directly to the IT skin under loose-fitting cloth trousers. Results from this study were consistent with previous studies, showing monotonic changes in temperature from foam type cushions, decreases in water floatation, and non-significant changes in gel pads, even at a two-hour interval period [55, 76].

Foam tends to increase cushion interface temperature because their construction materials and air within are poor conductors of heat [19]. Gels and viscofoams tend to have high heat transfer, and exhibit almost passive cooling before the body of material reaches equilibrium with the ambient temperature and seated individual. After about 2 hours, this initial heat capacity is saturated, and pressure relief lifts must be taken or a heat will continue to accumulate in a manner similar to standard foams. Microclimate of fluid cushions is affected by the specific heat of the fluid material contained in the support surface [19].

In a study utilizing a thermodynamic rigid cushion loading indenter (TRCLI), cushion types were evaluated by composition with respect to temperature and local relative humidity. The TRCLI approximates the seated microenvironment of a human in a standardized and repeatable manner [58]. This study classified each cushion type as either a high/low dissipater of both heat and moisture. Foam cushions were on the low end of heat but higher end of moisture dissipation. Viscofoam cushions showed low heat and moisture dissipation, whereas gel cushions were high heat, low moisture [58]. Air cushions were closest to the cutoff between high and low heat dissipation, with poor performance with respect to moisture [58].

2.2.4 Summary

Foam cushions are the relative baseline cushion composition; this material does not exhibit marked ability to redistribute pressure, shear force, interface temperatures, or relative humidity. It is easy to manipulate for customization (contours, segments, etc.), which could be beneficial in the development of a modified cushion to house site-specific cooling elements. Viscoelastic foams are similar in performance to standard foams, offering temperature-dependent immersion and envelopment levels, time dependent pressure redistribution, unremarkable handling of shear and initial resistance to changes in interface temperature; prolonged exposure to high temperatures elicit steady increases over time. Air cushions perform well with respect to pressure redistribution, but this performance is dependent on appropriate initial inflation. They resolve shear forces well and have good heat dissipation qualities, although are poor dissipaters of moisture.

2.3 MEDICAL AND COMMERCIAL COOLING EQUIPMENT

Currently existing strategies to lower body temperatures were evaluated in addition to cushion construction materials. Studies involving commercially available devices, support surfaces, and personal cooling devices are detailed below in order to ascertain the advantages and disadvantages of each cooling modality.

2.3.1 Rapid hypothermia induction techniques

Induction of both mild and severe hypothermia has been used as an intraoperative therapy for the reduction of cerebral ischemia, hypoxia, cardiac arrest, and many other conditions [77-80]. The effective principles of core body temperature reduction could be applied to local cooling elements. The simplest method of hypothermia induction is the application of ice or cooled gel packs to the head, neck, and torso of a patient, providing a slow ($0.9^{\circ}\text{C}/\text{hour}$) cooling rate compared to more advanced systems detailed below [81]. Cooling blankets have been utilized and demonstrate core temperature decreases of $1 - 2^{\circ}\text{C}$; these devices circulate cold water through tubing or embedded chambers by a pump. Blankets are wrapped about the patient, in direct contact with the skin [81, 82]. One novel device (Thermosuit system, Life recovery Systems, Kinnelon, NJ) utilizes the speed of direct immersion in ice-water bath by circulating a thin layer of ice water within a narrow plastic membrane encasing the skin [83]. This same concept is utilized by several forced air or circulating water mattresses, although these mechanisms of cooling are generally large and utilize a standard refrigeration module and fan/pump for circulation [78].

Other methods involve using pre-cooled materials with high thermal conductivity that are fixed to the skin surface in a variety of ways. EMCOOL's (Emcools, Vienna, Austria) pads are small, adhesive patches of a thermally conductive plastic placed directly on the skin surface, and provides a rapid cooling rate of 3.3°C/hour [84] in acute cardiac arrest. A later study by the same research group utilized cold metal plates pre-cooled to -20°C fixed to swine skin by silicone webbing [85]. While highly effective in lowering body temperature, these methods require pre-cooling, storage of replacement pads or plates, and lose cooling capacity relative to ambient temperature.

2.3.2 Personal cooling systems

Personal cooling devices (PCD's) have been developed to alleviate the strain associated with warm ambient climates or during strenuous activities such as military combat, firefighting, chemical processing, exercise, or strenuous labor. PCD's are generally garments such as vests, scarves, and hats which function from either passive cooling, circulated fluid (water, air), pre-cooled thermally conductive or heat reflective materials. In a comparison of air-cooled to water-cooled vests by Shapiro et al., internal and external temperatures were monitored during strenuous activity in full military uniform [86]. Both vests demonstrated roughly equal (90W) cooling power in high humidity environments, based on calculations derived from Givoni and Goldman [87]. Both systems achieved skin cooling through evaporation of sweat, and results were highly dependent on ambient air temperature and relative humidity. Subjectivity to ambient environment of liquid cooling garments were confirmed by later studies using dry or sweating thermal manikins [88, 89]. Cooling vests were proven to be ineffective in lowering overall body temperature in hyperthermic athletes after heavy exercise [90], and proved just as

effective or even less effective as hydrating with cold water for combat marines in simulated tasks [91]. A variety of passive cooling PCD's were utilized to examine the effects of heat on work tolerance time, comfort level, heart rate, and core temperature on red pepper harvest workers [92]; while results were highly favorable, cooling capacity greatly diminished roughly one hour after initiation. Rotating out, "recharging" or allowing these passive PCD's to reach normal ambient temperatures away from the body restored their effectiveness.

2.3.3 Cryosurgical devices

Cryosurgery (the application of very low temperatures to tissue) has been used in a variety of medical fields including dermatology, oral, retinal, heart, and liver procedures [93]. Recent applications of two cooling and heat transferring devices have possible applications towards a targeted skin cooling element. The first was the development of an instrument used to freeze small areas of skin for wart removal. It consisted of a system which delivered local cooling through the use of thermoelectric coolers (TEC). TEC's utilize the Peltier effect to generate a temperature differential between two dissimilar metals. If a current is passed through these two materials, "heat is either absorbed or released at the junction, depending on the direction of the current flow" [94]. Thermoelectric coolers offer the advantages of standard refrigerant systems without the complicated pipes, hoses, motors, and circulating fluid accompanying it. The biggest challenge in TEC systems is the removal of the heat generated at the warm junction, opposite the side removing heat. Generally these devices are coupled to a heat sink or radiator to be cooled by ambient temperature, circulating fluids, or forced air. The aforementioned device was able to achieve an applied temperature differential of 45°C using a two stage, fluid cooled system. A second device combined the cooling capacity of thermoelectric coolers with a heat pipe at the

application area to deliver cooling at the tip of a probe. Heat pipes transfer heat with very high efficiency (several hundred times higher than most metals), and consist of “closed, evacuated envelopes, in which a working fluid (whose vapor pressure is at a desired operating temperature) evaporates and condenses due to volume expansion of the phase change. The working fluid then moves back from the condenser to the evaporator by means of capillary action through a specially designed wick material” [93]. While heat pipes are nearly ideal heat transfer materials, they also are subject to orientation limitations (as the wicking material is limited when working against gravity) and specific operating ranges relative to the working fluid within.

2.3.4 Summary

A summary of the variety of available options currently used to cool skin or core temperature in clinical settings was compiled; methods which were most feasible and advantageous to meet both technical and user needs were detailed in Table 1 below:

Table 1: Advantages and disadvantages of cooling methods

Cooling Method	Advantages	Disadvantages
Water bath	Fast cooling rate High heat capacity Most effective temperature drop in literature	Difficult to contain Limited time before recooling No closed loop control
Fans and blowers	Can be used in many orientations Capacity for closed loop temperature control	Air exchange required Heat transfer dependent on evaporation Noise Dust / moisture buildup Requires power source Difficult to cool well below ambient
Heat Sinks / Passive Cooling Materials	Can be used in many orientations Easy to implement No moving parts	Functions only to a particular range of temperatures Limited time before recooling No closed loop control unless coupled with another system Requires precooling
Compressor-based cooling	Capacity for closed loop temperature control Cooling below ambient Cooling large amounts of heat	Maintenance of moving parts Noise Requires power source Size
Water circulating with heat exchanger	Capacity for closed loop temperature control High heat capacity	Condensation Leaking / hoses Less heat removal Limited by heat sink Requires power source
Air circulating with heat exchanger	Capacity for closed loop temperature control	Dependent on relative humidity / sweating Heat transfer dependent on evaporation Limited by heat sink Requires power source
Heat pipes	High thermal conductivity No moving parts No power source required	Limited by orientation No closed loop control unless coupled with another system
Thermoelectric Coolers	Can be used in many orientations Cooling below ambient No moving parts Small Size Temperature control	Limited by heat sink Requires power source Selection of TECspecific to desired max temperature drop

2.4 DESIGN SPECIFICATIONS

Various design tools were useful to organize the assessment of current standards of care, support surfaces, and cooling methods for the design of a cooled cushion. By detailing the functional requirements, constraints, limitations, and available materials, decisions were made regarding the incorporation of features into potential solutions. The quality function deployment (QFD) method is a “team-based method that draws upon the expertise of the group members to carefully

integrate the voice of the user” in the design process [28]; this method was useful in organizing and structuring features of the design and benchmarks interpreted from the literature. The house of quality (HoQ, Table 2) for product planning represented a graphical method to list wheelchair cushion user (“customers”) needs next to the various engineering characteristics of our project goals. Engineering characteristics are generally defined by some physical unit or subjectivity measure. By associating the end user needs with the technical requirements, our group was able to discuss, understand, and come to consensus on important details of the cushion design.

Table 2: House of Quality Matrix

Customer Needs	Technical Requirements																											
	Ambient temp. operating range	Ambient humidity operating range	Pressure Range	Weight of cushion	Area of local cooling	Material heat transfer properties	Rate of cooling delivery	Average Battery Life	Recharge Time	Noise level	Time to reach target temperature	Setup and operation time	Variation in applied temperature	Voltage Requirements	Cyclic loading lifetime \ durability	Target Skin temperature	Target Skin Relative Humidity	Meets CMS coding for adjustable skin protection cushion										
Stability			X															X										
Minimized Friction and Shear Force	X	X	X										X		X			X										
Redistributes Interface Pressure			X															X										
Targetted Skin Cooling to Reduce Interface Temperature					X	X	X				X		X			X												
Portable				X																								
Long Battery Life								X	X					X														
Quiet									X																			
Comfortable	X	X	X					X	X							X	X	X										
Easy to use											X																	
Compatible with current wheelchairs				X	X													X										
Durable														X														
Suitable for wide variety of users	X	X	X		X		X									X	X											
Washable/cleanable															X			X										
Lightweight				X																								
Adaptable to various cushion sizes																		X										
Technical Requirement Units	°C	% RH	mmHg	kg	mm ²	W/m ²	°C/min	hours	hours	dB	min	min	°C	V	years	°C	%RH	CMS code										
Technical Requiriement Targets	37	22	5	99	18	70	160	100		2	645		4	8	12	10	7	10	40	35	15	5	±1	12	3	25	min	E2605
Technical Requiriement USL	0	37	5	99	18	70	160	100		2	645		4	8	12	10	7	10	40	35	15	5	±1	12	3	25	min	E2605
Technical Requiriement LSL	0	37	5	99	18	70	160	100		2	645		4	8	12	10	7	10	40	35	15	5	±1	12	3	25	min	E2605

As seen above, the HoQ matrix consists of the user requirements, technical requirements (with their associated units and safety limits), and marked by any interaction between them. Both

needs and requirements were determined from the literature and interviews with field experts and wheelchair users. HoQ diagrams are often populated with numerical correlation ratings assessed from surveys or other data sources, although this analysis was deemed unnecessary for our purposes in generating initial design solutions. The QFD illustrated the important features to focus on, including: maintaining skin protection properties, comfort, meeting daily usage requirements (battery life), and adjustability to a variety of users and wheelchair settings. An engineering design specification sheet (Table 3) was then created to summarize the findings of our initial design phase; this living document evolved as solutions were conceptualized, evaluated, and in some cases, prototyped and tested.

Table 3: Engineering design specifications

Title: Cushion with site-specific temperature control for pressure ulcer prevention.

Introduction:

Design problem: need cushion capable of point cooling areas at highest risk under seated individual

Intended purpose: Reduce the temperature at the skin-support surface interface to increase skin tolerance to pressure.

Unintended purpose: Pressure redistribution

Customer requirements:

- Skin should be cooled to temperatures around $25 \pm 1^\circ\text{C}$.
- Battery life and heat sink capacity should be able to run 8-12 hours at a time to satisfy daily wheelchair cushion use.
- Must overcome human body heat generation of 64-244 W/m^2 (resting-heavy activity).

Operating environment:

- Wide variety of ambient temperatures ranges and relative humidity.
- Should tolerate incidental exposure to moisture.
- Cooling effectiveness should be variety of users' seated skin temperatures.

Economic:

- Economic life of three to five years. Wear and tear dependent on activity level of user.
- Should not require servicing outside of routine cleaning.

Geometric limitations:

- Cooling mechanism should fit within currently existing support surface dimensions.

Reliability and robustness:

- Low failure rate during activities of daily living on a support surface.
- Fail safe system to prevent over-cooling or undesirable operation.
- Able to respond to changes in interface temperature (closed-loop control of cooling).

Safety:

- Skin should not be exposed to hot or heated portions of the device.
- Should not overcool skin to cause cold damage or appreciably lower core temperature.
- Cooling mechanism should not reduce support surface's ability to redistribute pressure or introduce a pressure focal point.
- Low voltage requirement < 50V.

Pollution:

- Will not create noise > 30-40 db.

Human factors:

- Support surface designed to fit 95th percentile females and males.
- Simple mode of operation, 'out of the box' usage.

3.0 CONCEPT & CONFIGURATION DESIGN

The conceptual design phase followed the aforementioned QFD and engineering design specification development. Sketches, modeling, bench top experiments, and proof of concept prototypes were crucial steps towards developing our current and effective design iterations. Concept design refers to the process by which “alternative design concepts are distinguished as embodiments of physical principles, materials, or geometry. They are evaluated for feasibility and/or preliminary performance.” A wide variety of cooling methods were summarized in 2.3.4 and the two most effective means to cool a cushion interface were selected for this design phase. Circulating water and thermoelectric cooling systems were chosen because of their ease of implementation, high heat capacity, and ability to be controlled based on feedback from the system. Configuration design is where the overall architecture or components of a solution are analyzed, synthesized, and arranged [28]. This process was carried out to refine the second design concept, whose preliminary performance met the needs specified in the QFD and the targets of the design specification.

3.1 WATER CIRCULATING SYSTEM

The first interface cooling method attempted was circulating cooled fluid through a network of tubing impregnated in a standard foam block cushion. We began with a large-scale model to

gauge feasibility and make observations to fine tune the design concept. A standard foam cushion was chosen because of ease of modification, availability, and relatively good ability to dissipate pressure. This feasibility layout, diagrammed in Figure 2, consisted of a fan-cooled radiator block, circulating motor, flow speed controller (Gigabyte Inc., New Taipei City, Taiwan), foam cushion, in-series flow temperature monitor (Thermaltake Inc.), and power supply. Flexible tubing of 13mm diameter, 1.5mm thickness allowed cooled water to circulate across the surface of the cushion. Heat generated beneath the test subject would be conducted through the tubing to the water, which then passed through the radiator cooled by a variable speed fan. Both the fan speed and circulating pump were thought to have an effect on the cushion cooling performance. The water circulating system was adapted from a CPU liquid cooler, which supports chips operating from a 60-80°C range.

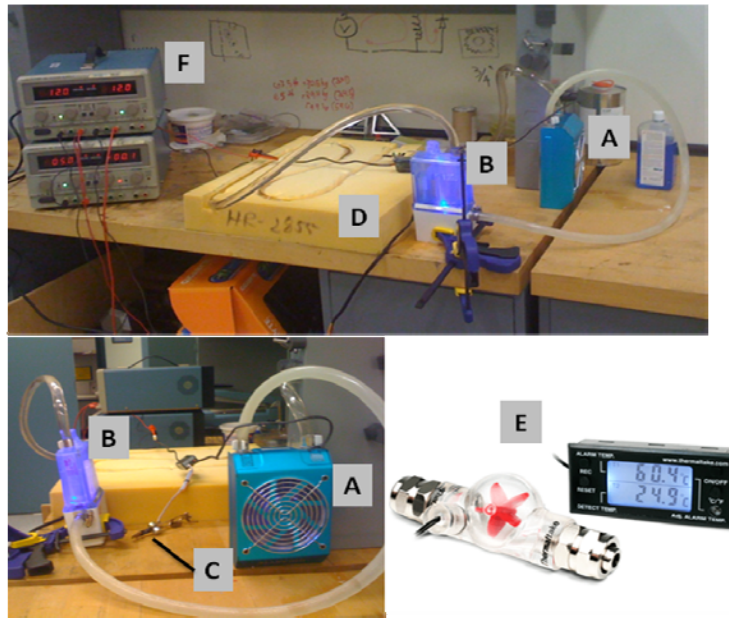


Figure 2: Diagram of water cooling system. (A) Fan-cooled radiator. (B) Water circulating motor. (C) Flow rate adjustment knob. (D) Foam block cushion with inlaid path for water tubing. (E) In-line water temperature monitor. (F) Power Supply.

The foam block was then outfitted with several thermistor probes (Cole-parmer Models U-08502-14, U-08443-20) illustrated in Figure 3 without a seated user on the cushion. The cooler ran for approximately 30 minutes prior to any pilot testing in order to allow the water to reach constant temperature ($22 \pm 3^\circ\text{C}$). A volunteer test subject sat in standard cotton scrub pants during 45 min trials, with temperatures recorded every 15 min under both ITs and thighs. Ambient temperature was $23 \pm 1^\circ\text{C}$, with roughly 18% RH. At maximum water circulation and fan speeds, initial seating tests showed no appreciable difference in temperature throughout the trial, and temperatures actually increased from an average of 25 to 34°C at each location after 45 min. This was thought to be attributed to the thermal insulation of the foam block as well as the thickness and spacing of the tubing. Another point to note was that there was condensation occurring at the cushion interface at and around the cooled tubing. These (and other benchtop results) data were not statistically analyzed.

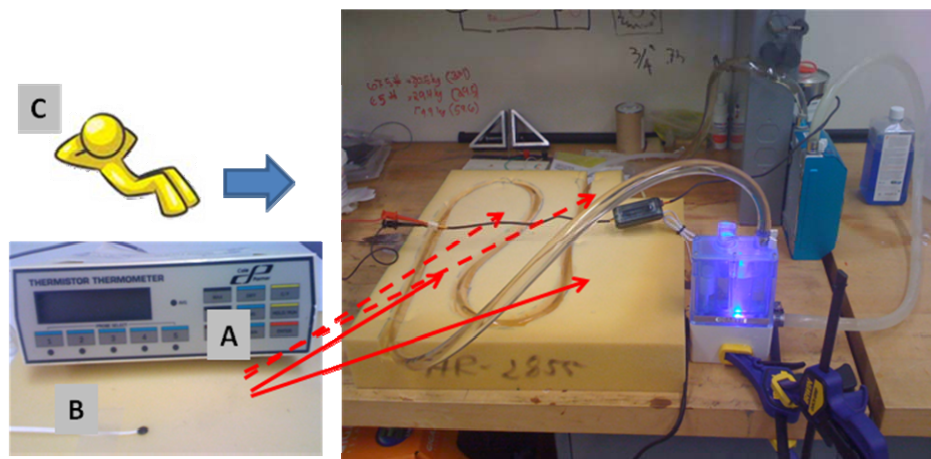


Figure 3: Thermocouple sensor locations - (A) Thermistor scanning module. (B) Thermistor. (C)

Orientation of seated test subject on cooling concept.

The layout of a commercially available seat cushion cooler which circulated water through a thermoelectric cooling (TEC) block was then examined in a similar manner. The heat generated by the TEC units was conducted to a pair of heat sinks which were cooled by fans.

Reduction of foam thickness, decreasing the layout spacing of the tubing within the foam, and lowering the tubing dimensions to 6mm diameter, 0.5mm thickness (Figure 4) was equally ineffective in lowering interface temperature. Temperatures did not *increase* past 32°C but were not reduced towards the target protective range described above. Moisture buildup also continued to be a common problem during full-length trials.

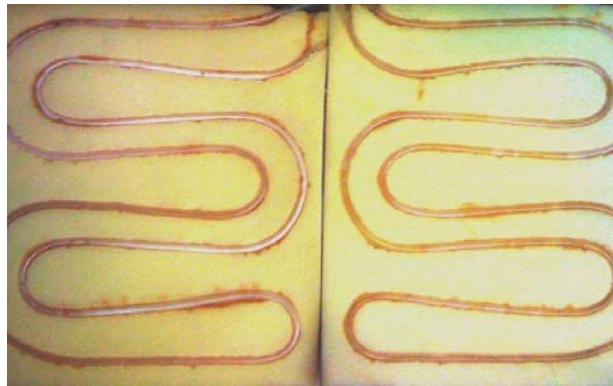


Figure 4: Modified tubing layout, reduction in tubing wall and foam thickness.

3.1.1 Analysis of design

It was concluded that using circulated fluid to cool the surface of a foam cushion was an ineffective means of providing local cooling. Several key issues included:

- The system itself was cumbersome to assemble, arrange, and utilize.
- None of the layouts achieved the target interface temperature.
- The water volume needed added appreciable weight to the cushion.
- Managing the tubing to avoid kinking was challenging.
- Several of the moving parts and components required electric power.
- Variability in fan speed, water circulation speed, tubing length, thickness, and material selection all lead to changes in performance.

- The system was not resistant to changes in ambient temperature.
- Condensation occurred along the length of tubing.
- A large cooling area which did not focus anatomic locations most at risk of pressure ulcer development.

To increase effectiveness, the design would require a reduction of moving parts, lower condensation, and more defined points of contact cooling. A previous study conducted in our lab utilized a thermoelectric cooling (TEC) module to apply local cooling at the sacrum, and maintained it using a small fan and heat sink [20]. Several of the challenges from the previous design iteration could be solved by imbedding a thermoelectric cooler within a cushion, properly removing the heat generated across the junction, and aligning those coolers with areas most at risk for pressure ulcer development. A problem with this approach is that seating a person directly on a stiff thermoelectric cooler would introduce a substantial pressure gradient. TEC's are housed in metal or ceramic plates in various sizes, and must also be accompanied with a heat sink, also made of thermally conductive materials. These components would interfere with a cushion's ability to provide immersion and envelopment if imbedded directly below bony prominences. A medium at the interface with the buttocks which transfer cooling yet meets sufficient pressure requirements would be required.

3.2 DESIGN OF A THERMOELECTRICALLY COOLED AIR CUSHION

3.2.1 Product layout - Air cushion with thermoelectric elements

3.2.1.1 Design layout

A segmented air cell cushion technology provides solutions to several of the challenges listed above and was selected as the core technology for this design. The ROHO single chamber high profile air cushion (ROHO Group, Belleville, IL) is classified by CMS as an adjustable, skin protection cushion [95] and provides suitable redistribution of pressure, shear, and interface temperature as discussed in 2.2.4. The overall construction of individual cells allows for site-specific additions of interface cooling elements. Segmented air cell cushions, such as the ROHO shown in Figure 5, use a system of cells interconnected by channels that allow air to flow at a controlled rate from cell to cell. As this occurs, the bony prominences are immersed and enveloped in the cushion material, increasing the contact area and distributing the applied force on the buttocks. A properly inflated segmented air cushion will allow a person to sink to roughly 0.5” of clearance between the buttocks and the bottom of the cushion [71]; the internal pressure of the cushion supports the applied load of a seated person. Thermoelectrically cooled cushioning elements could be incorporated into this clearance space of the air cushion.



Figure 5: Example of multi-cell ROHO air cushion

The project team postulated that gel pads or blocks could serve as the interface between small thermoelectric devices and the seated individual. There are several benefits to this approach; first that a soft, contouring gel pad would have better contact with the skin and allow the cooling to be delivered more effectively. Second, the cushioning effect of the gel can protect the user from the force applied when the user sits upon these thermoelectric coolers rather than the cushion of air in the clearance space. Third, the cooled area would be limited to the zones immersed farthest into the cushion, corresponding to the anatomical locations at high risk for developing pressure ulcers. This cooling element design is modeled below in Figure 6.

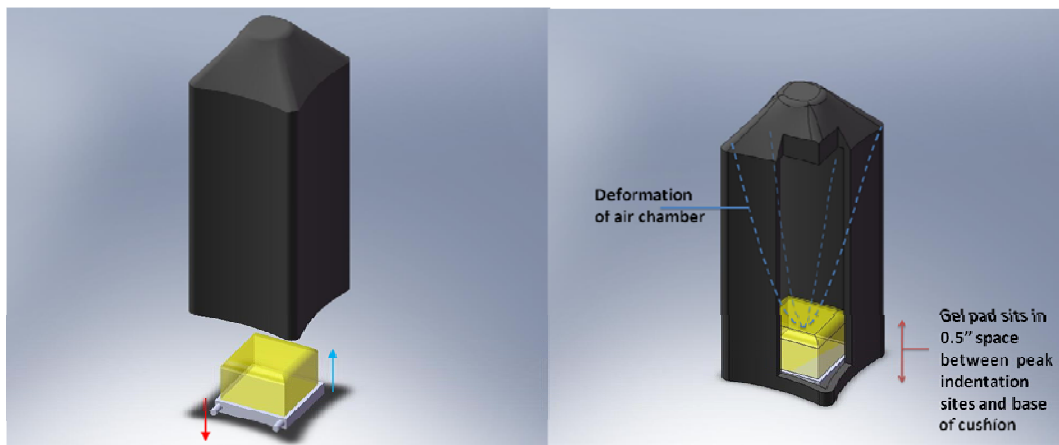


Figure 6: (Left) - Exploded view of cooling element. (Right) - air cell under load.

Individual cooling elements can be inserted through the base of the cushion into the individual air chambers. The gel pad is positioned atop a thermoelectric cooler and the chamber resealed around the TEC using neoprene epoxy to maintain the internal pressure of the cushion used to support load. The hot side of the TEC is fixed to a heat sink to draw the generated heat away from the TEC and gel pad. As the air cells deform, the buttocks would come in contact with the gel pad, which is cooled by the thermoelectric cooler situated at the base of the cushion. These cooling elements could be arranged in arrays throughout the cushion depending on the needs of the user (Figure 7). Different zones beneath a user could be individually controlled and

calibrated to cover small or large areas of targeted cooling. For the purpose of design development and evaluation, a single cooling element was developed, tested, and optimized.

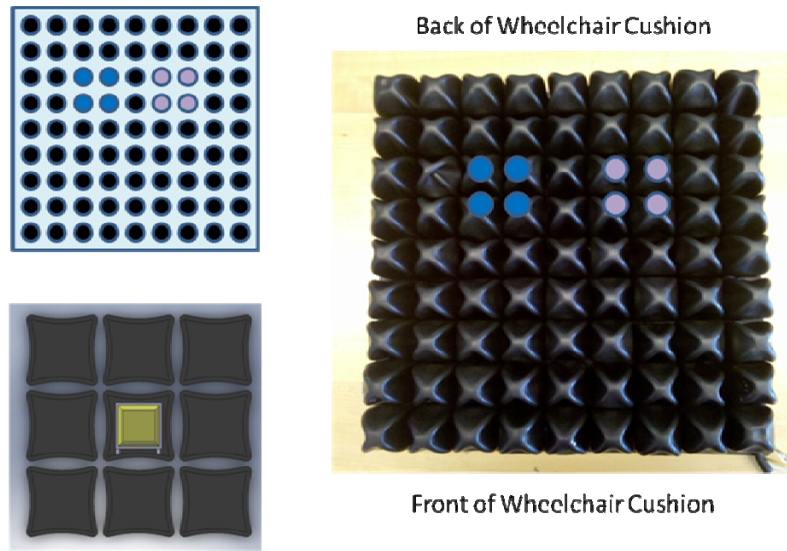


Figure 7: Potential arrangement of cooling elements within a cushion.

3.2.1.2 Component summary

A prototype cushion was fabricated using the aforementioned design and is detailed in Figure 8. The single chamber, high profile ROHO cushion (model: 1R99C) (A) sat atop a support frame (G) whose height accommodated the heat sink (E) and cooling fan (F). The heat sink was machined from aluminum to a 76.2x63.5x63.5 mm block (3x2.5x2.5 in.) and has a basic fin design (spaced 2 mm apart) to allow convection to dissipate the heat created by the TEC. Aluminum 6061 was used due to its thermal properties and ease of machining (specific heat Al 6061: 0.896 J/g-°C, thermal conductivity: 167 W/m-K). A Hengshan (Hengshan Group, FS70252M, Taiwan) CPU cooling fan was oriented perpendicular to the fins with the design of increasing convection to ambient air. The gel pad (B) was set into the base of a ROHO air cushion located where the left IT was expected to be immersed into the cushion. Figure 9 shows

several views of this design; the dashed representation of the buttocks illustrates the alignment of a seated user on the model and prototype images.

The initial gel pad used for prototype construction was provided and designed by Pittsburgh Plastics Manufacturing Inc. who partnered with our laboratory towards the completion of this project. The gel pads first supplied were glycerin hydrogels bound in 0.8mm urethane film, approximately 12.7x25.4x12.7 mm (0.5x1x0.5 in.), and press fit into the base of the Modified ROHO. The gel pad was designed to cool approximately 645.16 mm² (1 in²) while in contact with the buttocks.

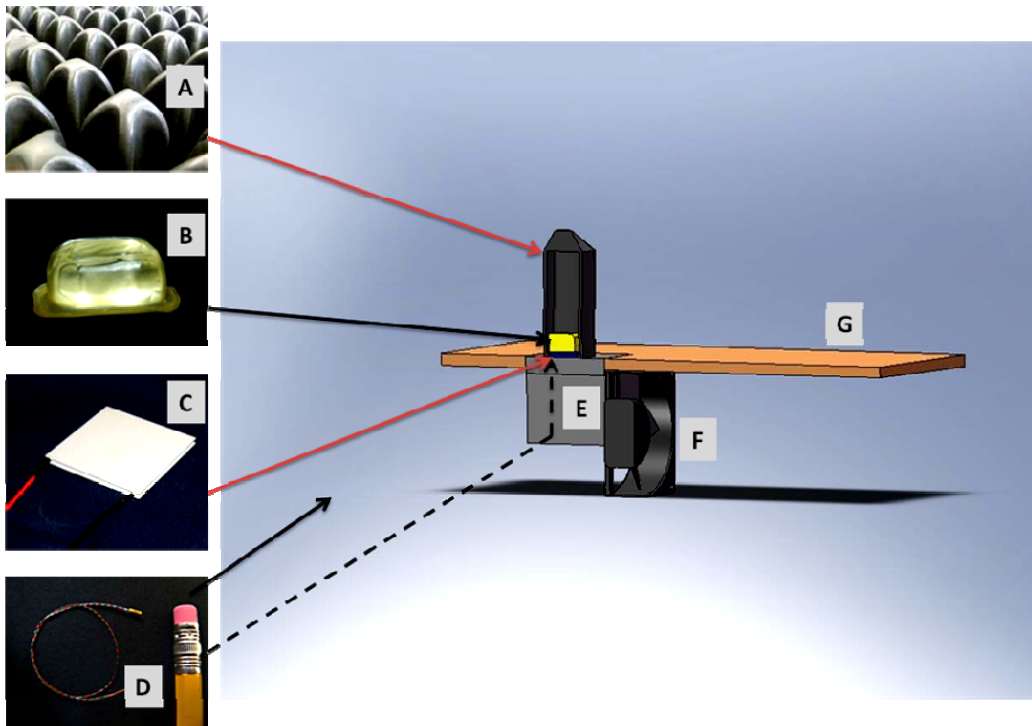


Figure 8: (A) ROHO air chamber. (B) Thermally conductive gel pad. (C) TEC unit. (D) Sensing and control thermistors. (E) Heat sink. (F) Heat sink cooling fan. (G) Support platform and frame.

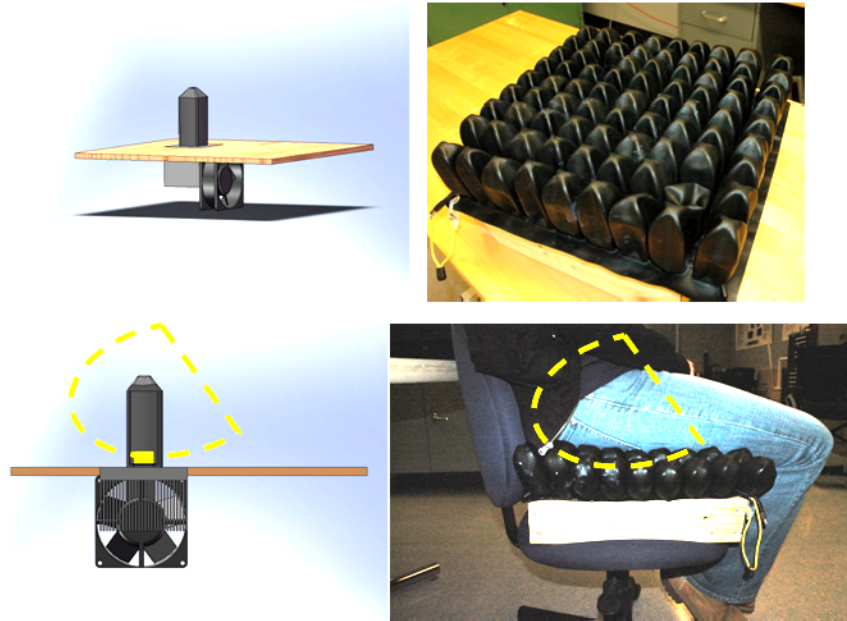


Figure 9: Model and physical layout of cushion design

The interface between the gel pad and TEC module was coated in a thin layer of thermal grease (Thermal Joint Compound, Wakefield Thermal Solutions, Pelham NH) to increase heat conduction. For this first design iteration, the gel pad was exposed to the cushion interface without the neoprene material of the ROHO air chamber covering it (Figure 10). In this manner a seated user would be exposed directly to the cooled gel pad. The border surrounding the severed air chamber was sealed with airtight thermal epoxy (Royal Adhesives & Sealants, LLC, Belleville NJ). This prevented any appreciable loss of air pressure. The air chambers surrounding the thermoelectric cooling unit provided adequate support to allow a seated person to come in contact with the gel pad without bottoming out.

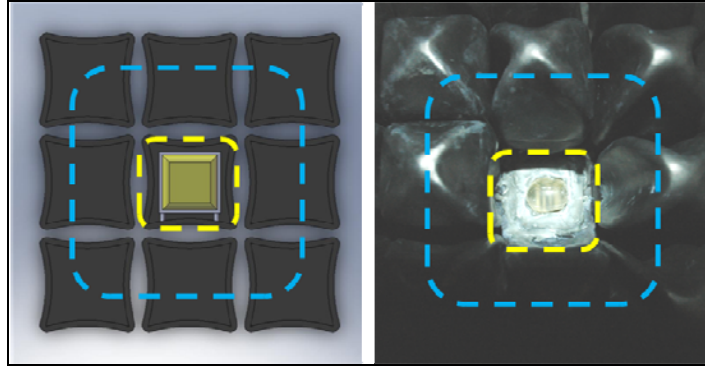


Figure 10: Epoxy sealed border to prevent air loss (yellow) and supporting air chambers (blue)

3.2.1.3 Instrumentation

A closed-loop thermoelectric cooling control system (TE Technology, Traverse City, MI) was used to keep skin interface temperature at approximately 25°C. The thermoelectric cooler (C) (TE-71-1.0-1.3) and heat sink were attached using a press fit and thermal grease. Two thermistors (MP-2444) were placed in the system to monitor interface temperature and send feedback to the temperature control board (TC-36-25-RS232). The feedback control thermistor was imbedded within the gel pad, and the interface thermistor was placed between the seated participant and the cushion itself. The placement of these thermistors is detailed below in section 3.2.1.5. The control board (Figure 11) is a device that controls the voltage and the current that is delivered to the TEC by receiving commands from a nearby computer (see Appendix A for full wiring diagram). The controller utilized a proportional-integral-derivative (PID) control scheme to maintain the temperature of the TEC. The board was controlled from a Labview program (Version 8.6, National Instrument, Austin, TX) which transmitted all parameters of the controller program (Figure 12, Figure 13). The program was capable of recording temperature vs. time data in ASCII files and displayed the controller and interface temperatures in real time.



Figure 11: TEC controller board with two power supplies (A)(B) and dual input thermistors (E)(F).

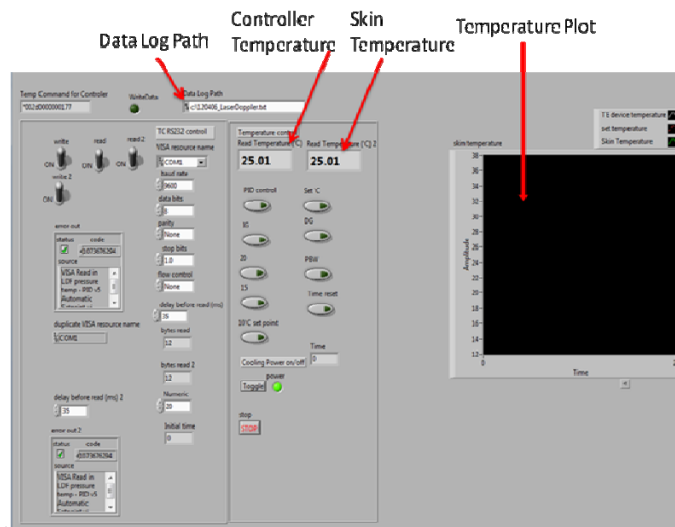


Figure 12: Labview control program GUI

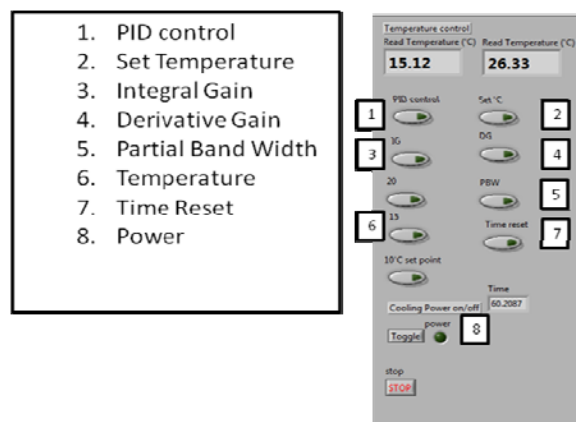


Figure 13: Labview control button labels

3.2.1.4 Air pressure setup procedure

In order to seat persons on the cushion in a repeatable manner, a cushion inflation protocol was established based on the methods used in Brienza et. al [96]. This assured that the person seated on the cushion was properly supported and in good contact with the thermoelectrically cooled gel pad for all evaluation trials. A trained occupational therapist provided guidance and training to the research team for this task.

The ROHO cushion was calibrated by overinflating the air cushion and then allowing it to reach environmental pressure with the air valve open. The subject was then lowered onto the cushion in a normal seated posture with the valve closed; care was taken to align the TEC unit with the IT of the seated person in the transverse plane. The investigator then slid a hand between the cushion surface and the seated person, feeling for the lowest bony prominence. Air was released while the investigator kept their hand under the person until there was approximately 0.5” of clearance between the base of the cushion and the surface of the buttocks just over the ischial tuberosity. This was generally just enough room for the investigator to slide their fingers out from under the cushion on the unmodified side. The IT on the modified side of the cushion was confirmed to be directly above the imbedded cooling element by palpation. Inflation was checked periodically throughout each testing procedure to ensure the user had not bottomed out. Bottoming out refers to when a seated user comes in unsupported contact with the base of the cushion due to insufficient internal air pressure.

3.2.1.5 Gel pad and controller configuration

Optimal use of the PID controller depended upon the location of the sensing thermistor that would give feedback to the system for the closed loop control. Possible locations (Figure 14) included (A) within the supporting gel pad, (B) atop the supporting gel pad, (C) below the gel

pad directly in contact with the thermoelectric cooler, and (D) outside the cooling element on the skin of the seated individual. In addition, the set point towards which the controller drove the thermoelectric cooler in response to the measured interface temperature had yet to be determined. In the previous studies at our lab [20, 21], the controller was provided a set point of 25°C to provide local skin cooling. Initial bench top experiments with the prototype cushion demonstrated that a 25°C set point would be insufficient to reach the target protective interface temperatures at the skin.

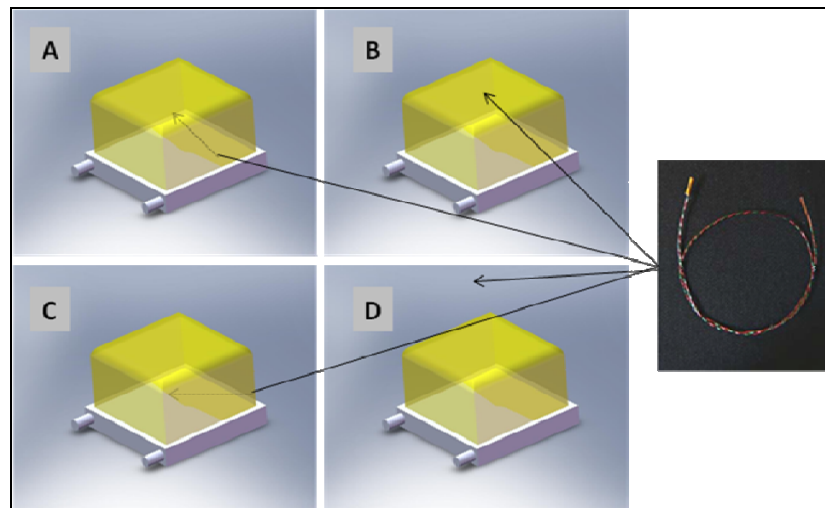


Figure 14: Control thermistor test locations. (A) Within gel. (B) Above gel. (C) Below gel in contact with TEC. (D) On skin of seated user.

To evaluate the effect of location and set point on interface temperature delivery, the following experiment was conducted using the hydrogel sample from PPM. The goal was to determine which experimental setups would approach $25 \pm 1^\circ\text{C}$. The highest temperature set point possible was preferred, since the TEC requires proportionally more power and generates more heat as the target temperature decreases. The conditions tested were 20, 15, and 10°C temperature set points. The control thermistor locations investigated included within the gel pad, atop the gel pad, and between the gel pad and TEC (illustrated in Figure 14A, B and C).

Thermistor control at the skin (Figure 14D) was not evaluated as it was deemed impractical for standard everyday use of a functional cushion.

We used an additional interface thermistor to measure the temperature between the seated user and the cushion in the same manner as Sprigle et. al [97]. This sensor was for data collection purposes only and had no influence on the control of power supplied to the TEC. This thermistor was placed between the user's IT and the gel pad; the IT location was confirmed by palpation. Users sat directly on the exposed hydrogel pad as the neoprene cushion material was removed for the cell containing the cooling element. Subjects wore cotton scrubs and undergarments for each experiment.

Prior to the test, the cooling system was not active and the cushion and gel pad were exposed to ambient temperature ($23 \pm 3^{\circ}\text{C}$, RH $20 \pm 5\%$) which remained relatively constant throughout each trial. Two volunteer test subjects were used for this analysis to obtain five repeated trials for each control thermistor location/TEC temperature set point condition. These subjects remained seated after being positioned on a properly inflated modified cushion as described in section 3.2.1.4 for hour-long intervals. The controller was activated through the Labview program as either participant settled onto the cushion. Both interface and controller temperatures were monitored continuously throughout the tests at 20 Hz.

For each test condition, interface temperature data for all trials (5 trials / condition) was averaged over approximately 25 seconds (500 data points) and is displayed in Figure 15. It was clear from the experiments that placing the control thermistor on the surface of the TEC was an ineffective feedback location for the interface temperature sensor. A 20°C controller set point was also insufficient to bring the interface temperature below 27°C ; this trend was evident during early testing trials inside the gel and on the TEC, and so this temperature state was not tested

atop the gel pad. The most successful trials were 15 or 10°C set points with the control thermistor placed within the gel pad (Figure 14A) or on top of it (Figure 14B). As stated above, the set point and location with the lowest power requirements and generated heat would be selected for use in all future tests. **A set point of 15°C combined with the control thermistor within the gel effectively produced an interface temperature of 25° ± 1 °C** (max stdev = 0.85°C during steady state). The TEC temperature also oscillated at 15 ± 0.2°C, which demonstrated the control board was operating within its appropriate bandwidth (Figure 16). We estimated that at average throughput the cooling system ran at approximately 20W. It should be noted that starting temperature of both the skin and gel pad was not controlled for this series of experiments; each trial tended to reach a steady state temperature at t = 900 sec (15 min), and it was from this point in time forward that the evaluation criteria was applied. The small interface temperature fluctuations were caused by subject movement (e.g., leaning, shifting) during trials.

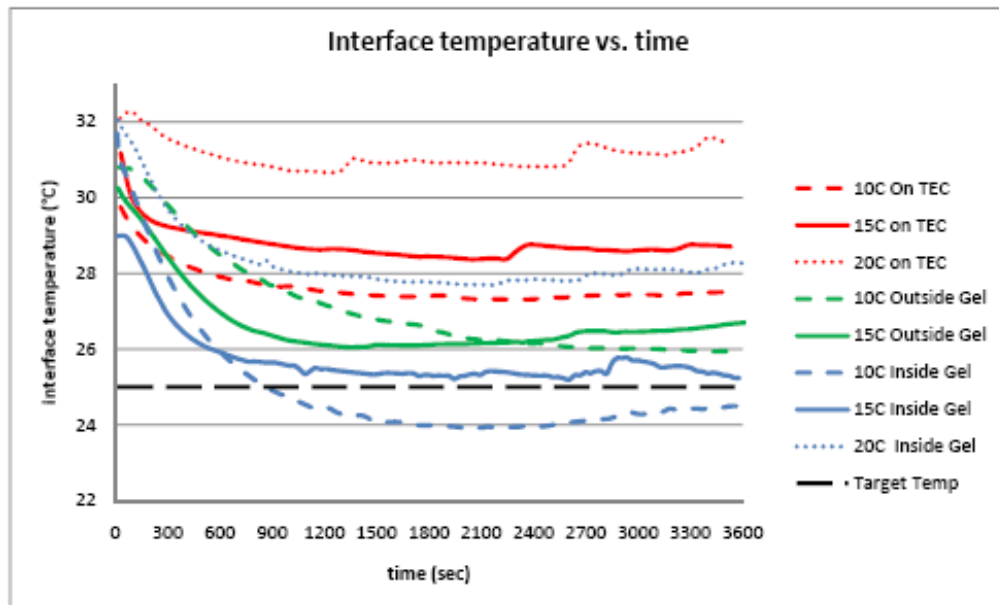


Figure 15: Plot of interface temperature vs. time for various combinations of control thermistor location and TEC set point temperature. Values averaged over 5 trials, every 500 data points. 20C on top of the gel pad was not tested.

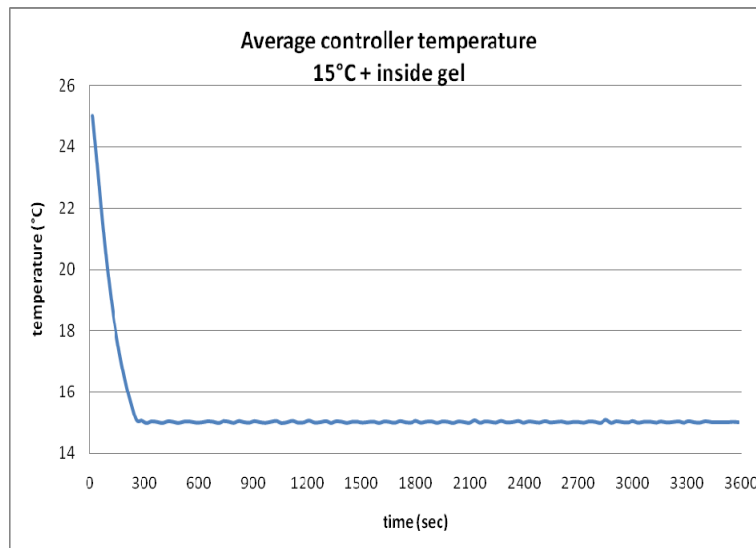


Figure 16: Control temperature oscillation about set-point.

3.2.1.6 Selection of gel pad materials

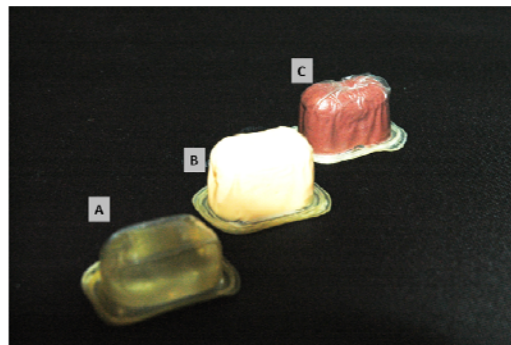
Early benchtop experiments with readily available materials such as water pads, gels, ice packs, and comfortT foam (Otto Bock, Burlington, ON, Canada) proved unsuccessful in terms of thermal transfer between the TEC and cushion interface. A local plastics company, Pittsburgh Plastics Manufacturing (PPM), aided us to utilize novel materials for our gel pad. PPM provided us with two additional gel samples in addition to the hydrogel used for design layout and controller development: polyurethane gel modified with ceramic microspheres and polyurethane gel with resin microspheres (Figure 17). Each material was designed to maximize thermal conductivity while still providing adequate cushion support at the buttock interface. Example thermal conductivities provided by PPM are listed in Table 4 relative to a commonly used metal for heat conduction. The hydrogel pad's thermal conductivity was closest to that of glycerin (0.28 W/m*K) as this was its primary aqueous component, while the modified polyurethane gels' conductivities would be higher (~0.4 W/m*K).

Table 4: Example thermal conductivities of gel pad materials relative to copper.



Material	Thermal Conductivity (W/m*K)
Copper	401
Water	0.58
Glycerin	0.28
Polyurethane	0.02
Mod. PolyUreth	0.4

A series of tests were conducted on the two polyurethane with the same procedures listed in sections 3.2.1.4 - 3.2.1.5. The control thermistor was imbedded within the pad, and the controller was set to drive the TEC towards 15°C. Each gel pad material was tested for 1 hour duration over 5 repeated trials. For analysis, trials were averaged every 25 seconds (500 data points) and the change in temperature with respect to their initial temperature calculated. Figure 18 shows that the hydrogel material exhibited the largest temperature difference (< -5°C) and closely approached our target interface temperature of 25°C.



**Figure 17: Gel pad materials - (A) Hydrogel, (B) Polyurethane modified with ceramic beads
(C) Polyurethane modified with resin beads.**

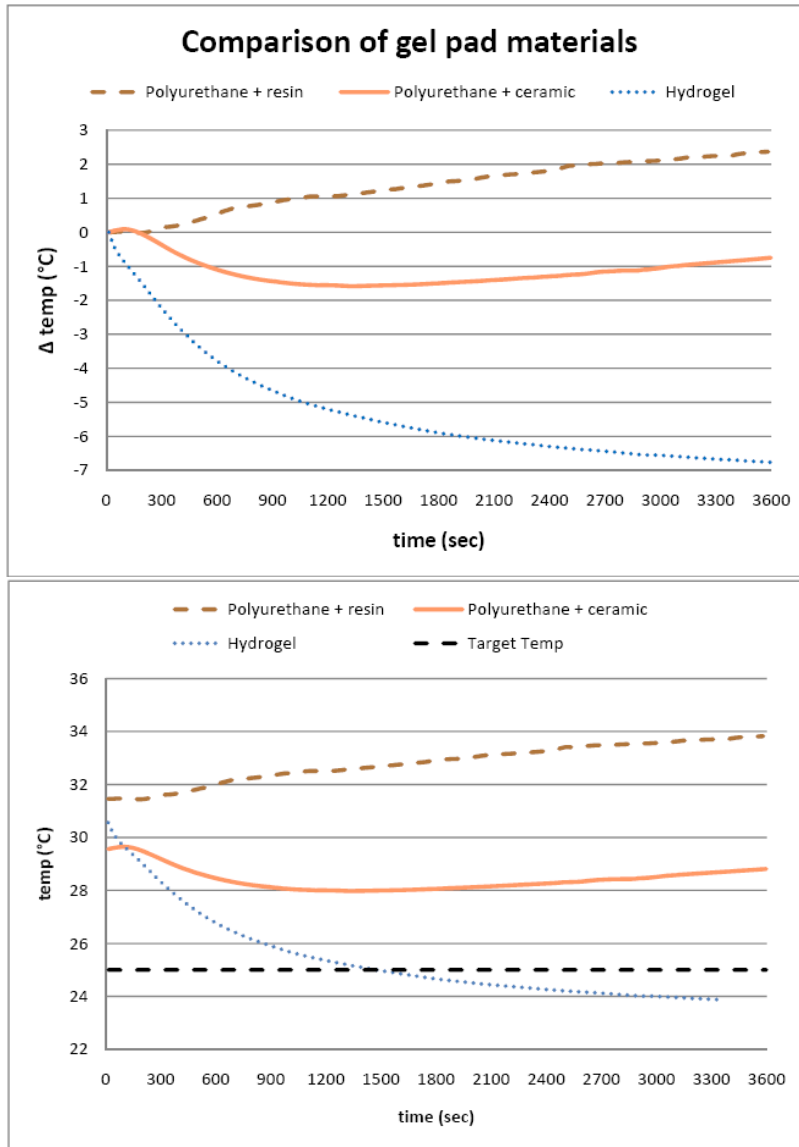


Figure 18: Change in interface temperature from starting temperature (top) and absolute (bottom) interface temperature of gel pad materials.

3.2.2 Component refinement - Air cushion with thermoelectric elements

Following component analysis of the control parameters, thermistor locations, and gel pad materials, the following changes to the design were implemented towards the completion of the prototype. These changes were largely the result of moving towards a more functional cushion,

anecdotal experience while testing the previous design iterations, and optimizations for more efficient heat transfer, both at the gel pad and heat sink interfaces. As stated above, a 15°C controller temperature setting was utilized to achieve 25°C at the interface. Control thermistors were imbedded within the hydrogel cushioning pad for feedback of local temperature (section 3.2.1.5). Version 2 of the prototype air cushion with imbedded thermoelectric elements also utilized the following:

3.2.2.1 Increased hydrogel pad size

We increased the size of the gel pads from 12.7 x 25.4 x 12.7 mm (0.5x1.0x0.5 in.) to a slightly larger 25.4 x 25.4 x 19.05 mm (1x1x0.75 in.), as shown in Figure 19. Often times during experiments slight weight shifts or leaning would cause the gel pad to lose contact with the locally cooled area, resulting in observable temperature spikes at the interface. It was thought that by increasing the height and width of the gel pad, more continuous contact would be maintained with a seated user. Moreover, the polyurethane membrane binding the gel pad was removed to increase thermal transfer between the TEC, gel pad, and application site. A small 25.4 x 25.4 mm (1x1 in.), 0.8 mm (.03 in.) thickness square of polyurethane was placed on the top layer of the gel pad to prevent adhesion to the ROHO neoprene during use. The new gel pads fully occupy a ROHO air chamber but left enough clearance to allow air redistribution between neighboring cells.

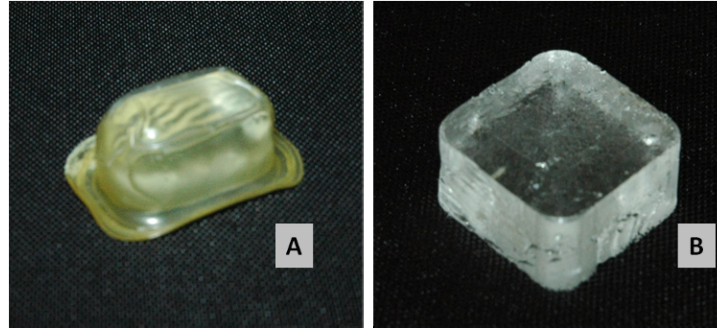


Figure 19: Comparison of first (A) and second (B) generation hydrogel pads.

3.2.2.2 Fully enclosed air chamber design

Figure 10 illustrates how the previous design removed the modified air chamber completely in order to press fit the gel pad into the ROHO cushion. This forced the user to rely on the neighboring air cells to redistribute applied sitting pressures above the cooling element. In the second design iteration, we removed material from the underside of the cushion only. The void left by removing the base neoprene (Figure 20A) was then filled with a larger gel pad, which was held in place by compressive forces and secured using Neo-rez neoprene epoxy (Wahoo International Inc., Oceanside CA) (Figure 20B). After curing, the control thermistor was punctured into the body of the gel pad, and a small amount of epoxy was used to secure it in place. Finally, the unit was covered in thermal grease to facilitate heat transfer to the TEC unit aligned below it (Figure 20C).

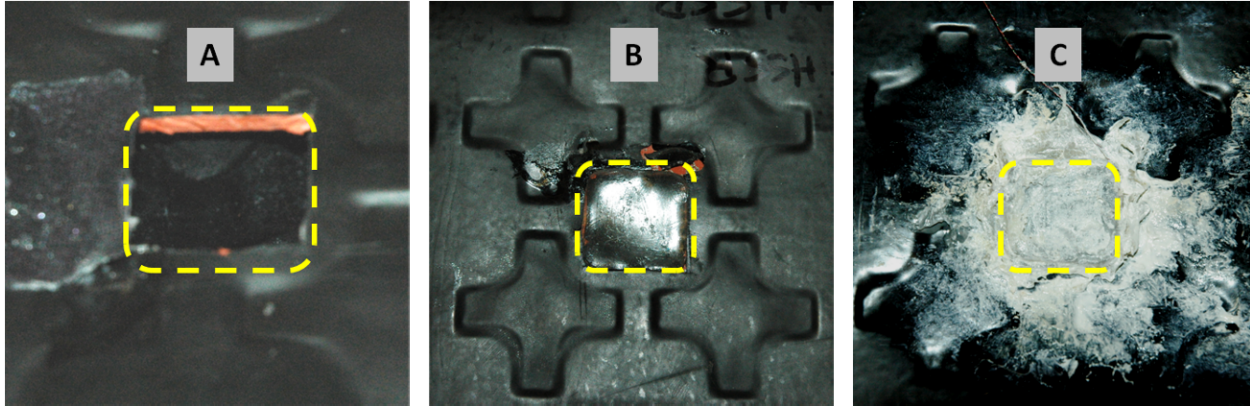


Figure 20: Underside view of gel pad secured in ROHO air chamber.

3.2.2.3 Revised layout

In order to increase comfort and demonstrate feasibility of the prototype on a standard manual wheelchair, the support base of the cushion was modified to fit a 16"x17" Quickie (Breezy Ultra 4) wheelchair frame (Figure 21). A drop seat platform was machined to accommodate the aluminum heat sink below a seated user. A cooling fan from Delta Products (SFB0212HH-F00, Fremont CA) was aligned perpendicular to the orientation of the fins to increase convective heat transfer (Figure 22). This fan offered a wider cooling area with dual rotors and dimensions that matched those of the heat sink. The fan and heat sink were aligned where our modified, single chamber ROHO's cooling element would rest in a normal seating position. The complete system (cooling element, heat sink, fan, and control board) added 1.05kg to the manual wheelchair.

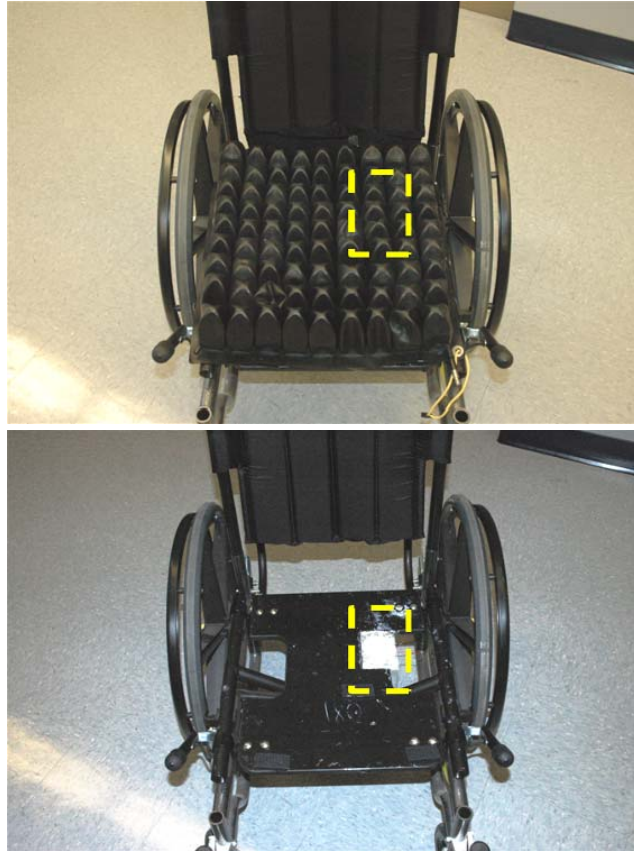


Figure 21: Quickie wheelchair with and without modified ROHO cushion.

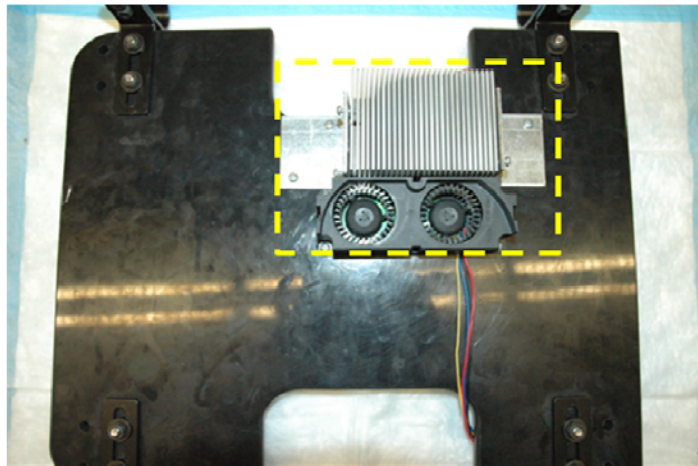


Figure 22: Underside of machined drop seat illustrating mounted heat sink and cooling fan.

4.0 PROTOTYPE EVALUATION METHODS

To evaluate the second generation prototype of the air cushion with thermoelectric cooling elements, experiments were designed to assess the cushion's ability to deliver appropriate levels of cooling, adequately redistribute interface pressure, and provide sustainable cooling over a day of wheelchair cushion use. These studies were 'proof of concept' in nature, and are therefore not necessarily hypothesis driven. Their outputs are derived in order to evaluate the current design features of the cool cushion. As such, no outside participants were enrolled nor IRB approval required for this study due to the nature and scope of any participants evaluating the cushion. Two healthy males (aged 20-30) similar in height, weight, and body composition, volunteered for these cushion evaluation studies. Subjects were able bodied and not screened for specific diseases, or restricted from medications, food, or drink prior to the start of any evaluation.

4.1 ADDITIONAL INSTRUMENTATION

4.1.1 Thermal imager to measure interface cooling

In addition to the instrumentation listed in section 3.2.1.3, thermal images were acquired for 7 pairs of trials in order to verify local skin temperature resembled the temperature measured with

the interface thermistors. Temperatures were recorded non-invasively using a Fluke Ti20 Thermal Imager (Fluke Corp., Everett, WA). The manufacturer's reported accuracy is $\pm 2\%$ or $\pm 2^\circ\text{C}$ (whichever is greater).

4.1.2 Force sensing array to measure pressure redistribution

Interface pressure measurements were recorded throughout the tests using a Force Sensing Array (FSA) pressure mapping system (Vista Medical: UT1010-4307, Winnipeg, Manitoba, Canada). The FSA pressure mapping systems has a 16 by 16 array of paper thin, 25.4 x 25.4 mm (1x1 in.) sensors to measure and display interface pressures between the body and a support surface, measuring a maximum of 16in^2 . Peak Pressure Index (PPI) was used to quantify the interface pressure data. PPI is defined as “the average of the highest recorded pressure values within a 9-10 cm^2 area (the approximate contact area of an IT or other bony prominence). The number of individual sensels included in the calculation depends on the spatial resolution of the mat” [98], which in our case equals four. This measure has been shown to be more repeatable and reliable than average or peak pressure measurement in the literature [99]. The FSA software provides a visual output of the pressure data by showing numerical values with a colored overlay. These data can be exported to text files in order to extract numerical information, determine locations of high pressure areas, and to calculate PPI.



Figure 23: FSA pressure mat system.

4.1.3 Thermodynamic rigid cushion loading indenter to measure heat and water vapor transmission

A thermodynamic rigid cushion loading indenter (TRCLI) has been developed in order to simulate normal human conditions for sitting with respect to temperature delivery and water vapor. This work arose from the challenges surrounding simulation of local microenvironments of a support surface coupled with the increasing interest in the secondary risk factors associated with problems such as pressure ulcers. A full discussion of the development and function of this device is detailed by Ferguson-Pell et al. [58]. For the purposes of our study, this device was able to simulate the delivery of normal core temperature and relative humidity to our modified cushion (Figure 24). The body of the indenter is composed of a water tank, water vapor permeable membrane, capillary matting, and the polycarbonate shell (Figure 24). The sensor array on the outer shell of the polycarbonate section of the indenter consists of humidity sensors (SHT75, Sensirion AG; Staefa, Switzerland) and J type thermocouples.



Figure 24: TRCLI components

The sensors recorded data with onboard data loggers (National Instruments Field Point Modules 2015, FP AI-100, FP TC-100), which were accessed and controlled remotely by a Labview control program (Figure 25) and logged at 1 sample / minute. The sensors were fixed to the indenter at several anatomic locations on the underside, including the thighs, ITs, and perineal area. An external water circulator (NESLAB RTE-110) was used to circulate water at 4L/min, and $37 \pm 2^{\circ}\text{C}$. Ambient temperature was maintained at $23 \pm 2^{\circ}\text{C}$ using a standard room thermostat. Relative ambient humidity was increased to $50 \pm 5\%$ through the use of a MoistAir (HD14070) humidifier. An atmospheric temperature and humidity sensor (General Eastern) was used to monitor the ambient climate of the testing area. 500N of total force (including the weight of the indenter) was applied in each cushion test to simulate 78kg (~172 lb.) of body weight.

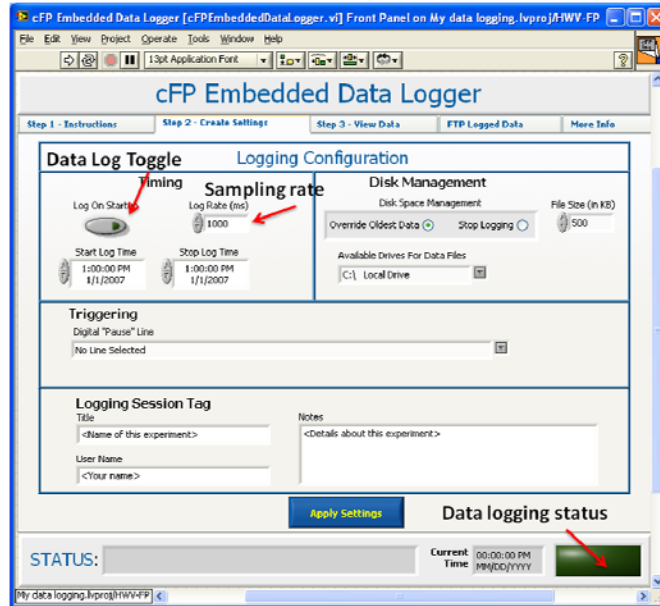


Figure 25: Labview controller for Fieldpoint data loggers

4.2 EXPERIMENTAL PROTOCOLS

4.2.1 Verification of interface cooling

For the study each participant completed 7 separate testing sessions. Each trial consisted of a 5 minute pre-test session and 60 min of temperature and pressure loading. Participants wore cotton scrubs and undergarments for each trial. If images were taken during the trial, the Fluke Thermal Imaging camera was mounted on a tripod and readied behind a privacy partition. Foot placement markings were clearly labeled with tape approximately 2m from the thermal camera in order to keep the subject in repeatable frame and focal distance. Images were taken of the bare buttocks to illustrate the area and local temperature as compared to the contralateral buttock.

During the 5 minute pre-test sessions the TEC cooler was not active and the cushion and gel pad were left at room temperature, which varied between 22-24°C and 18-22% RH (verified using a handheld temperature and humidity monitor). The cushion was then positioned on the Quickie wheelchair as illustrated in Figure 21 of section 3.2.2.3. The internal pressure of the cushion was calibrated according to the established protocol in section 3.2.1.4. Care was taken to ensure the seated participant's left IT was directly above the imbedded cooler, and that contact was present between the buttocks and gel pad. After the participant was properly seated, the cooler was toggled on via the Labview interface, and data was recorded for the interface and control temperature at 20 Hz. Test sessions were conducted for 60 minutes total as described by Brienza and Siekman [100] for air-filled cushions to observe when monotonic decreases tapered off and a steady state temperature could be observed. In trials where thermal images were captured, the camera was readied after the 60 minute trial and taken in the same manner as described above. This image was taken as quickly as possible (within 1 minute) to prevent normathermic processes and air convection from disturbing image repeatability. Three hours or more were allotted to allow the system to return to equilibrium between experiments.

4.2.2 Verification of pressure redistribution

For this comparison there were 2 subjects completing five trials on two separate cushions. Our modified prototype air cushion was compared to an unmodified high profile ROHO Quadtro cushion to investigate any difference in pressure redistribution measures. All air valves were opened on the Quadtro cushion so it could act as a single bladder high profile cushion. For this study, subjects were seated on either the TEC cooled cushion or the unmodified Quadtro in the Quickie Breezy wheelchair. Before placing the FSA pressure mat, the cushion was again

properly inflated using the methods described in section 3.2.1.4. When the cushion was calibrated the participant stood and the FSA pressure mat was placed on the surface of the cushion. Subjects were then lowered onto the pressure mat and interface pressures were observed on a nearby computer. Crimping or folding of the mat that occurred while sitting was adjusted by the research team prior to data collection. A loading time of 5 minutes was standardized to account for any potential creep effects on the interface materials, mat, or loaded tissue; this also allowed complete air distribution within the ROHO cushion to occur. Data collected at the 5 minutes marker were used to compute PPI for comparison of modified and unmodified ROHO cushions. Fifteen minutes were allotted to allow the cushions to reach equilibrium before further data was collected.

4.2.3 Heat and water vapor transmission

For this test we utilized an ISO standard draft protocol (CD 16840-7 Wheelchair seating, The determination of heat and water vapour dissipation characteristics of seat cushions intended to manage tissue integrity) which was modified for use with our cooled cushion[101]. The modification was the use of the manual wheelchair to support the cushion rather than a rigid platform. The specified testing environment of $23\pm 2^{\circ}\text{C}$ and 50% RH was maintained with environmental controls and an external humidifier; these conditions were verified by both a handheld temperature and humidity monitor and the onboard sensors of the TRCLI. Each heat and water vapor test ran for 3 hours and an additional 15 minutes following a short (45 sec) pressure-relief lift. For our purposes, we ran 5 trials and compared the modified and unmodified IT readings from each cushion test to verify delivery of cooling when compared to the contralateral side.

At the start of each experimental trial, the modified ROHO system was positioned beneath the indenter in a frame utilizing a pulley system to raise and lower the test jig (Figure 26). The capillary mat within the indenter was wetted with ~ 100mL of water to prime it for transmission of water vapor with a flexible pipette. The cushion was then overinflated as per the calibration procedure in 3.2.1.4. To begin data collection, the indenter was lowered onto the modified ROHO while data logging was active on both the fieldpoint module and thermoelectric control module through their respective Labview VI's. Care was taken to align the IT sensor array of the indenter with the air chamber embedded with the TEC via palpation. Air was released from the cushion under the weight of the indenter until appropriate air pressure was established (Figure 27). Once aligned, the cooler was toggled on and the system was permitted to run for 3 hours time. At the 3 hour mark a brief 45 sec pressure relief lift occurred with the TRCLI remaining roughly 100mm above the cushion. The indenter was lowered again, the sensors aligned, and data acquisition continued for 15 min. Data was later retrieved from the fieldpoint module via Ethernet FTP. Data points were extracted from the individual IT thermocouple and humidity sensor modules at: T_0 , T_{1hr} , T_{2hr} , T_{3h} , immediately following the pressure lift ($T_{3h+45''}$), and at the end of the trial T_F . Data from the same cushion on the contralateral side were used for comparison. Three hours were left between trials to allow the system to reach normal equilibrium before additional data was collected.

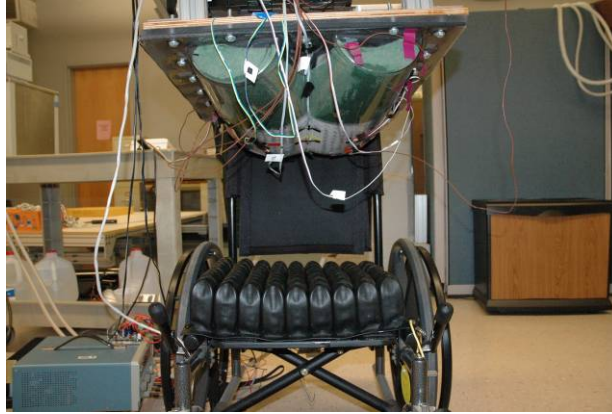


Figure 26: Modified ROHO and wheelchair base beneath TRCLI



Figure 27: TRCLI resting on calibrated ROHO cushion

4.3 RESULTS

4.3.1 Verification of interface cooling

The continuous temperature data was sampled from each trial ($n=14$) into five data points spaced 15 min apart. Data were found to be normally distributed using Kolmogorov-Smirnov (all $p > 0.01$) tests and plots of normality. We used single sample, two-tailed t -tests to compare the average value for each time point to our target temperature of 25°C . A p value of < 0.05 was

regarded as a significant difference. There was a significant difference in temperature value at the initial T_0 ($p = 0.026$) when compared to our target temperature. For the remainder of the time points T_{15} , T_{30} , T_{45} , T_{60} , no significant difference was calculated from our target temperature of 25°C ($p = 0.69, 0.36, 0.16, 0.29$, respectively). Figure 28 visually displays average values and 95% confidence intervals at each time point.

While not analyzed statistically, it is interesting to note some of the example thermal images taken before and after each cooling session. These images clearly demonstrated a distinct difference in skin temperature when compared to both pre-cooling images and the contralateral buttock following each test (Figure 29). Imaging offers several advantages over direct interface temperature measurement, which will be discussed further in section 4.4.1.

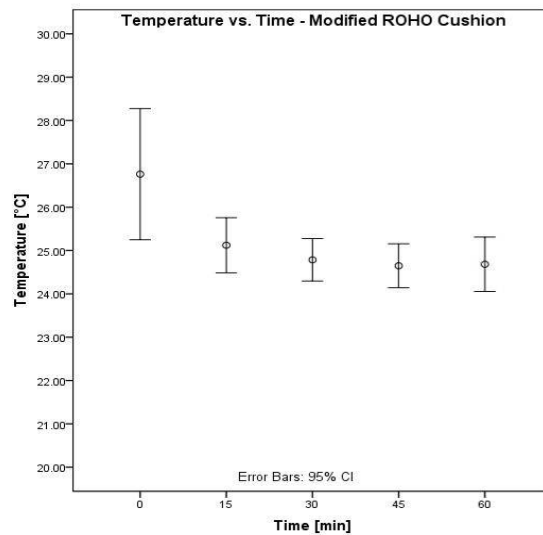


Figure 28: Average values at each time point with respective CI.

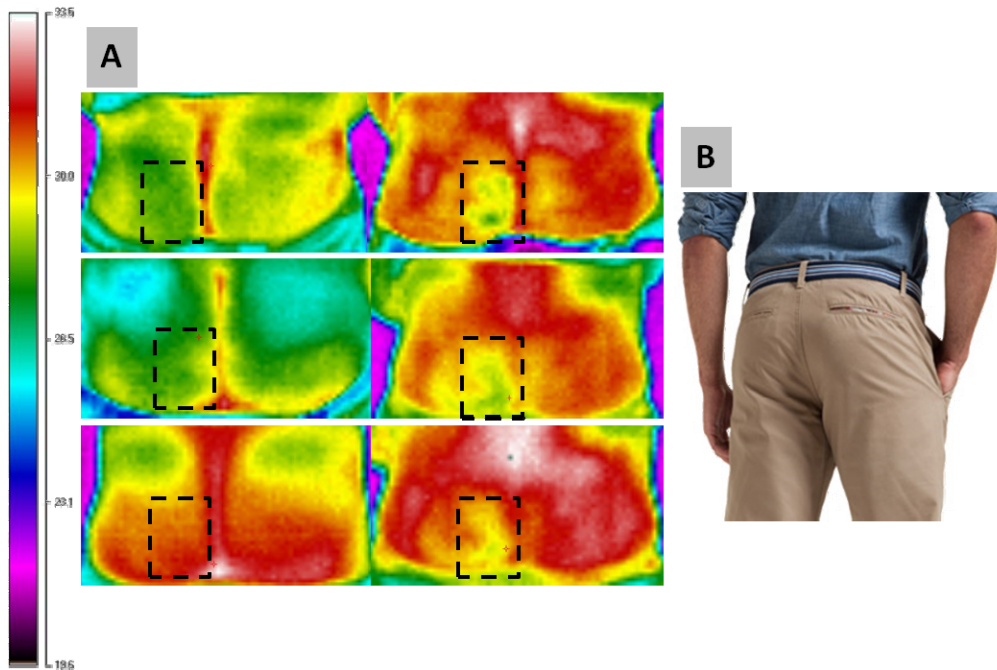


Figure 29: (A) Example thermal images (°C) before (left) and after (right) cooling trials. Dashed outline represents same area before and after cooling. (B) Thermal image orientation.

4.3.2 Verification of pressure redistribution

The pressure mat data was sampled 5 min after the start of the experiment to account for creep effects in the mat, cushion, and tissue being evaluated. Recorded frames were exported into excel and PPI was then calculated using a macro enabled spreadsheet. Average PPI for modified ROHO cushion was 64 ± 2.41 , where PPI for unmodified cushion was 63.20 ± 2.33 . Distribution was determined using Kolmogorov-Smirnov (all $p > 0.20$) tests and plots of normality. We used a paired, two-tailed t -test to compare the mean PPI for each both the modified ROHO and ROHO Quadro cushion. A p value of < 0.05 was regarded as a significant difference. There was no significant difference in peak pressure index ($p = 0.77$) between the two cushions.

Example pressure output data and box plots of calculated PPI for both cushions are illustrated in Figure 30 and Figure 31..

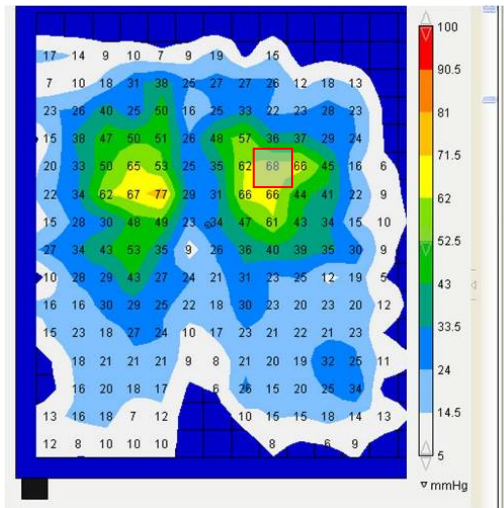


Figure 30: Example of pressure mat data. Location of cooler labeled in red over left IT region.

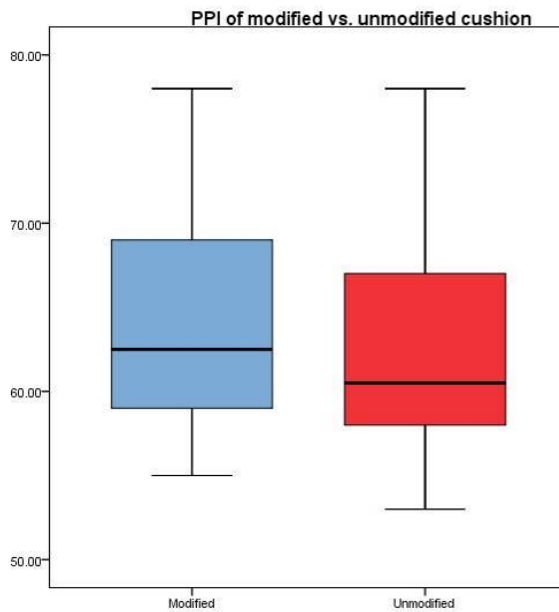


Figure 31: Plot of PPI for cushion comparison.

4.3.3 Heat and water vapor transmission characteristics

The heat and water vapor data was retrieved from the field point module and sampled at 7 points throughout each 3 hour trial, as detailed in [58]. Sensirion humidity sensor data were converted from voltage to humidity values using Equation 1:

Equation 1: Conversion of humidity input voltage to RH.

$$RH = \frac{((V/5) - 0.16)}{0.0062}$$

Comparisons were made between the cooled and un-cooled IT regions of the same prototype cushion. Distribution was determined using Kolmogorov-Smirnov tests and plots of normality. Paired *t*-tests were used for normally distributed data while the Wilcoxon signed rank test was used for nonparametric distributions to compare mean temperatures and RH at each sampled interval. A *p* value of < 0.05 was regarded as a significant difference. Average Temperature and RH for each side of the cushion is summarized visually in Figure 32.

There were no significant differences in temperature values between the contralateral sides for the first hour of testing (*p* = 0.20, 0.26, 0.13 for T_0 , T_{30} , T_{60min} respectively). Temperatures then diverged from 2 hours on and were significantly different throughout the remainder of the trial (*p* = 0.001, 0.002, 0.003, 0.002 < 0.05 for T_{120} , T_{180} , T_{181} , T_{196min} , respectively).

There were no significant differences in relative humidity values between the contralateral sides for the entire test session (*p* = 0.15, 0.62, 0.52, 0.60, 0.11, 0.38, 0.54 for T_0 , T_{30} , T_{60min} , T_{120} , T_{180} , T_{181} , T_{196min} respectively). RH data at T_{120} were not normally distributed so nonparametric tests of significance were used as described above. All data is displayed in Figure 33 to illustrate the high variability between trials.

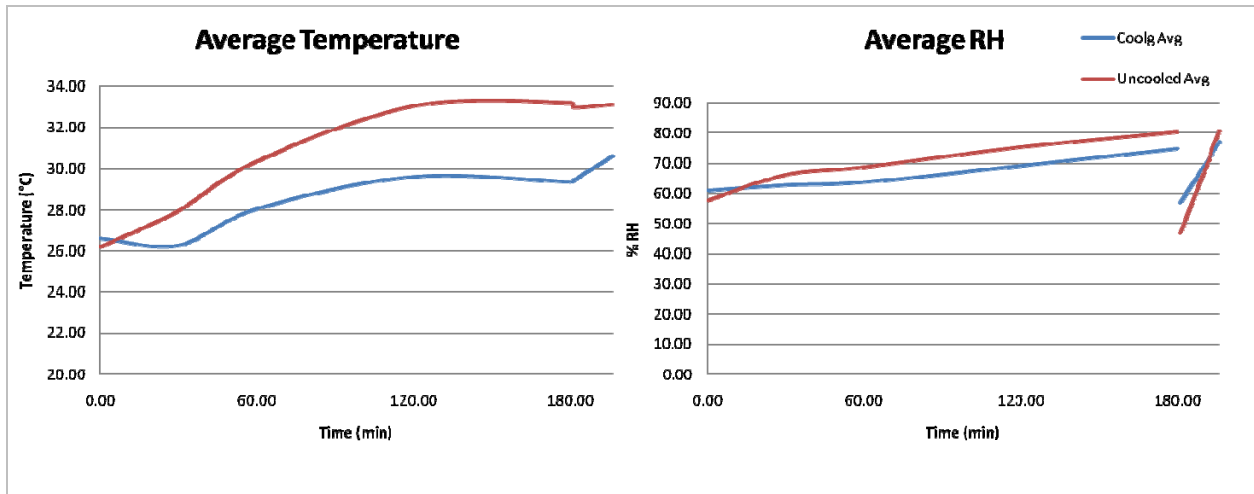


Figure 32: Average values for contralateral sides of cool cushion.

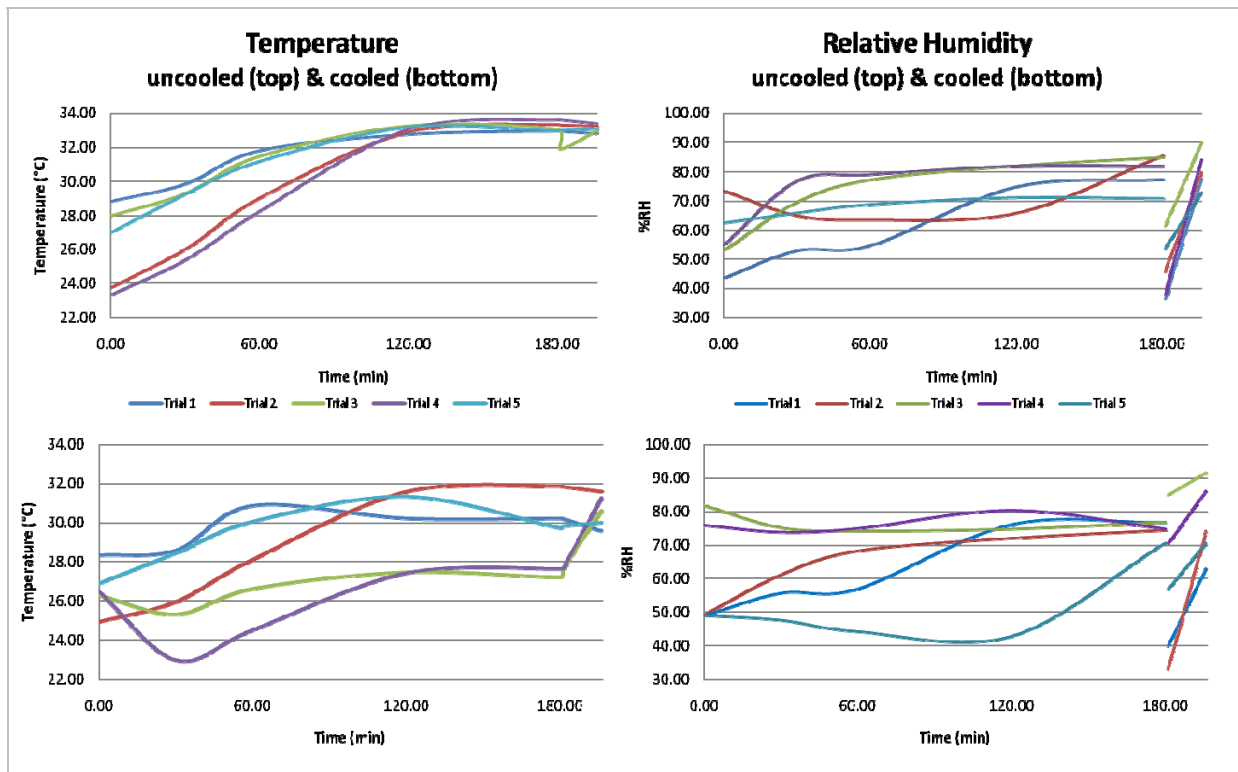


Figure 33: All trials for HWV characterization tests.

4.4 DISCUSSION

4.4.1 Verification of interface cooling

The series of temperature trials successfully demonstrated that achieving an interface temperature of 25°C and maintaining it for a sustained period of time is feasible using the thermoelectrically cooled system. Previous studies by Stewart et al. and Ferguson-Pell [75, 102] reported temperature increases of 7-8°C from baseline temperature on air support cushions after a 1 hour sitting duration. By this measure, without the cooling system active the cushion would be predicted to reach an interface temperature of 33-34°C after the hour long trial. The difference of 8°C would substantially reduce the locally cooled tissue's metabolic and oxygen consumption rate by a considerable measure (almost 46% based on the Arrhenius equation), as calculated by Lachenbruch in a summary of the protective effects of cooling at the skin-cushion interface [62].

Ambient temperature, activity level of the cushion user, inherent metabolic differences, and sitting duration before cooling trials could all account for the high degree of variability seen in initial temperature of the verification trials (T_0 , Figure 28). After 15 min of use, all trials were within the 95% confidence interval of our goal temperature, and stayed at this level for the remainder of our experiments. It should be noted that experiments challenging the cooling system in exaggerated hot or cold environments were not conducted. However, successful operation of this design was not dependent on any of the observed starting interface temperatures. Finally, while no time constant has been reported in the literature the protective temperature range could be induced rapidly using this design method.

Judy et. al. utilized a thermal camera system to record skin temperatures of patients at risk for pressure ulcers in conjunction with collecting the well established Braden Scale for the Prediction of Pressure Ulcers score [44, 103]. The hypothesis was that temperatures measured using thermal imaging of suspected or presented pressure ulcers would correlate well to a patient's Braden score. Images were taken at two anatomic sites: the sacrum and heel. The authors defined a temperature increase of 1.5°C greater than surrounding tissue as "at risk" based on Sprigle et. al [104]. The thermal camera system was able to more accurately identify high risk patients than nurses reporting Braden Scores alone, and all low risk patients identified by the images were also classified as low risk by trained nursing staff. We utilized a similar system to look at test skin temperatures as shown by the thermographic images in Figure 29. All images taken in this study showed a locally cooled area following the trial, although the absolute temperature measurements of the coolest areas from the camera differed from those reported by the interface temperature sensors. This can be explained by the time between when the trial ended and when the image capture took place; there is inherent restabilization of the skin temperature following exposure to ambient air temperature after direct contact with the cooler ceased. Tzen surmised that a 1.6°C increase in skin temperature followed local cooling at 25°C within one minute of removal [20]. The thermal imaging system is also limited to a reported accuracy of 2°C .

The interface sensor was placed on the surface of the ROHO cushion under the IT of interest, and therefore was not capturing *skin* temperature directly. However, a poster presentation by Sprigle et al. showed that on a ROHO cushion there was only a 0.3°C difference in temperature for skin versus cushion mounted sensors [97]. The thermal boundary between the skin and the cushion surface was reduced by standardizing the user's pant material during tests

and removing the standard ROHO cushion cover. The functionality of the cooling system could be impeded depending on a seated user's clothing in contact with the interface and/or the use of a standard cushion cover. A lower set point temperature would have to be calibrated in these cases to achieve the desirable skin temperatures. Although total cooled area was small, there exists no clinical or experimental guideline dictating the total cooled area, which results in the greatest level of skin protection related to local cooling. Future studies should investigate the relationship between cooled area and effectiveness of local cooling.

4.4.2 Verification of pressure redistribution

There were particular concerns with the impact of modifications to the ROHO cushion with respect to the cushion's pressure redistribution characteristics. Any positive intervention from providing local cooling would be equally offset if a pressure reducing cushion's capacity to redistribute interface pressure was compromised [105]. Moreover, some modifications could impart increased pressure points to an otherwise functional cushion. For the analyses, peak pressure index was calculated for our modified ROHO cushion and compared to a standard ROHO Quadro cushion. The ROHO Quadro cushion is readily available in the market and has been shown to be effective in redistributing pressure and preventing pressure ulcers in a recent RCT from our laboratory [25]. It is similarly coded for reimbursement as an adjustable skin protection and positioning wheelchair seat cushion [106]. An experienced seating specialist provided training and guidance for the calibration of the internal air pressure of both cushions used in this study. This critical step allowed a seated user to sink appropriately into the distributed air cushion for proper immersion and optimal load distribution. Using the same method as the aforementioned clinical trial, no statistical difference was calculated between the

cushion with the imbedded cooler and without, indicating no detectable pressure gradient was induced by the modifications of the single chamber ROHO cushion.

Peak pressure index was used to quantify interface pressure data because normal peak pressure measurements have been shown to be unreliable [98, 107, 108]. There are few reports in the literature for high profile ROHO cushions with which to compare our findings. An abstract by Sprigle et al. listed PPI for ROHO cushions from 0-20 months of use at 90-95 [109]. The PPI values reported in the comparative analysis were lower than these reported values at around 63-64 mmHg. These lower values observed might be explained by the careful setup procedure and control afforded to the test condition.

There was a detectable decrease in air pressure in the modified cushion over the course of use in the seated trials caused by a leak around the modified air cell. This leak was the result of an incomplete seal below the ROHO cushion where the hydrogel pad was inserted at the base. While steps were taken to properly reseal the cushion using epoxies and neoprene repair kits during assembly, general use and time were factors that gradually broke down this initial fixture. If left uncorrected, dangerously high levels of pressure similar to those observed when a user bottoms out on any standard cushion could result. Figure 34 below illustrates an intentional 'bottom out' in the ROHO Quadro (left), versus the pressure observed due to substantial air loss in the modified ROHO (right). It should also be noted that the modified ROHO was only equipped with a cooling unit below a single IT. Users had a tendency to bear down on the gel pad when improperly inflated; this was corrected with reinflation and verification of 0.5" clearance space as per the manufacturer's setup instructions [71]. However, this level of inflation could also subject the user to more direct contact with our cooling gel pad because of weight shifts or vibrations[108], resulting in a pressure node at the IT. In future prototypes,

reinforcing the seal around the gel pad or building the pad directly in as the cushion material is formed is recommended to get a complete seal and prevent any sensible air loss.

Finally, the change in *total* air volume temperature within the cushion was not studied in the verification trials. Substantial changes in temperature within each ROHO cell could increase or decrease internal pressure as the supporting gas expands or contracts. Future studies could address the severity of this effect on the overall cushion performance and whether these small changes in local temperature (and correspondingly, pressure) would put a user at risk for contacting the gel pad in a manner similar to Figure 34 (right).

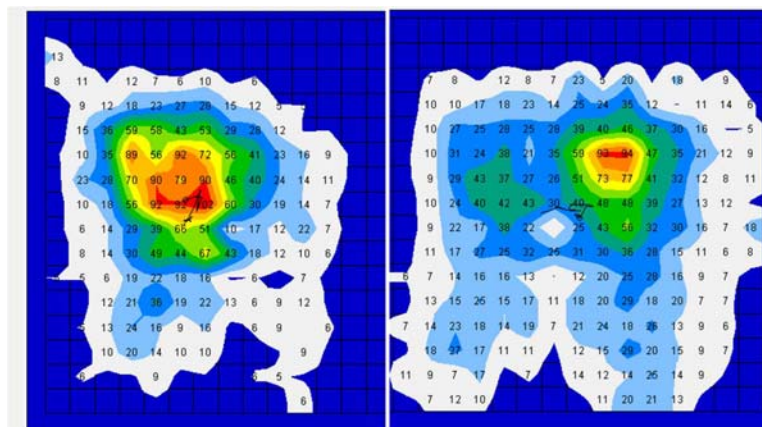


Figure 34: Examples of pressure mat readings. (left) bottoming out - (right) air loss

4.4.3 Heat and water vapor transmission characteristics

Ferguson-Pell et al. conducted a previous study in which the TRCLI was used to compare an unmodified ROHO cushion with various other cushion compositions [58]. Their goal was to group commercially available cushions by cover, core, composite material, or shape. One of the strongest correlations was that of interface temperature to core material. These previous findings were compared to those measured for the modified and unmodified sides of the ROHO in our

study (Table 5). In a general comparison, the unmodified ROHO measures were similar in magnitude to the previous measures with respect to temperature ($< 5\text{ }^{\circ}\text{C}$). The cooled cushion showed a 7.16°C and 5.89°C average drop as compared to the literature values at T_1 and T_2 , respectively. No discernible difference is shown with respect to relative humidity at any time point or difference measure. By their classification system, our modified air cushion would be listed as a high heat dissipater ($T_1 < 34^{\circ}\text{C}$) and low moisture dissipater ($H_1 > 60\% \text{ RH}$).

Table 5: Comparison of literature values to HWV test.

Cushion	Direct Measurement				
	T1	H1	T2	H2	T1-0
Ferguson-Pell	35.20	62.00	35.50	65.40	4.50
Unmodified	30.63	68.68	33.04	75.22	4.18
Modified	28.04	63.72	29.61	69.22	1.45
Cushion	Difference Measure				
	H1-0	T2-1	H2-1	T2-0	H2-0
Ferguson-Pell	19.80	0.30	3.30	4.80	23.20
Unmodified	17.77	2.68	6.54	6.85	8.46
Modified	2.74	1.57	5.50	3.02	8.24

* T = $^{\circ}\text{C}$, H = %RH

For the HWV trials, the cooled area of the cushion did not settle at 25°C as was observed in the temperature verification trials. This can be explained because the TRCLI is designed to deliver a constant rate of heat and water vapor regardless of ambient or local conditions; this is not the case *in vivo*. In general, local perspiration rate changes with skin temperature [110, 111], and the inhomogeneous makeup of local skin [112] would have a different thermal conductivity than a polycarbonate indenter to local cooling (muscle: $0.703\text{ W}/(\text{m}^{\circ}\text{K})$, fat: $0.116\text{ W}/(\text{m}^{\circ}\text{K})$, skin: $0.214\text{ W}/(\text{m}^{\circ}\text{K})$ [113], polycarb: $0.22\text{ W}/(\text{m}^{\circ}\text{K})$ [114]). The indenter also circulates water at 37°C and presents approximately 35°C at the cushion interface. This value is higher than any skin temperature we observed in 4.4.1 as well as literature reported values for clinical skin

temperatures near the buttock (min: 26.4°C, avg: 32.0°C) [104]. These clinical measures were taken at the *sacrum* and not at the IT, but represent typical skin temperatures 3-9°C lower than that of the TRCLI. Since the cool cushion control parameters were calibrated for delivery of 25°C, it was not surprising that the steady state temperature in the HWV trials did not decrease below 30°C. There was, however, a statistically significant decrease between the cooled and non-cooled cushion side after 1 hour onward, and the overall effectiveness of the local cooling was evident in the data.

A high amount of variation was evident across all cooling trials in the collection of both heat and water vapor data. We anticipated the temperature-time plots for all trials with local cooling to resemble those of the non-cooled side: similar in shape, heating/cooling slope, with similar end point temperatures. However, we instead observed a wide variety of responses to local cooling. This can be explained primarily because of the problems with capturing cooled data directly below the sensor fixed to the surface of the indenter. The testing protocol specified aligning the cooling element with the onboard thermistor and humidity sensor; this proved more challenging than aligning the interface thermistors in the skin cooling experiments since the seated user provided verbal feedback if they felt they were misaligned before each trial began. This problem is compounded by the loss of air pressure described in section 4.4.2, where alignment for initial internal air pressure would lose contact with the cooling element as air was depleted from the cushion.

The cooling elements had surprisingly little effect on relative humidity measures. No significant difference between average relative humidity at each time interval was observed. On average the drop in relative humidity was less pronounced than that of the uncooled IT during

the pressure relief lift ($T_{180}-T_{181}$). Our design goals were to meet specific local cooling levels and not necessarily designed towards reducing local relative humidity.

4.5 LIMITATIONS

There were several limitations to the experiments conducted to validate our cool cushion design. Data was collected on a limited number of subjects ($n=2$) and number of trials for each test selected was arbitrarily determined. Our data was intended to provide confirmation that the device met the targeted design specifications and goals. Data from these trials could be used to conduct a power analysis by establishing baseline values and variability for future studies aimed at determining the effects across a larger sample. Errors in data collection often eliminated additional trials which were not reported; however, these problems led to the development of more robust procedures and could then be translated into more reliable future studies.

One of the greatest challenges in data collection was capturing the cooled area of the cushion between the seated user and the thermoelectric cooling unit. This was due to the relatively small size of the sensing thermistors, and the tendency of seated participants to readjust, weight shift, or lean during seated trials. This is the inherent disadvantage of capturing the interface temperature under a thermistor of $<1\text{cm}^2$. The TRCLI offered similar challenges to monitoring temperature and humidity data. If sensors were not aligned, then the local cooling went unmeasured or poorly categorized. Moreover, while the TRCLI mimics *in vivo* boundary conditions, all tests were carried out in a carefully controlled environment. The influence of several factors such as individual variation in metabolism, sweating, and thermal characteristics of tissues were not accounted for.

Since the cushion modifications added appreciable weight to the manual wheelchair (1.05kg), this cushion design may not be desirable for manual wheelchair users. Implementing this solution on a power wheelchair would reduce the effect of the added weight and allow the system to be powered by the on-board battery.

Finally, this cushion prototype was manufactured using bench top methods, readily available materials, and previously existing cushions. It is not intended as a marketable product, but rather as a demonstration of the efficacy of imbedded cooling elements for targeted local cooling.

4.6 FUTURE DIRECTIONS

Future directions for this study could focus on three major areas. First, this cushion was equipped with a single cooling element near the left ischial tuberosity of a seated user. For future generations of this design the skin cooling units could be expanded to both sides of the cushion. The locally cooled area could be increased by adding an array of individually controlled TEC elements clustered around anatomic locations most at risk for PU development (Figure 7). Each element could be individually controlled and respond independently to local changes in microclimate. Future studies should clarify how many or how large a cooling area is necessary to provide adequate skin protection of the IT region.

Second, the cushion could be designed as a standalone system with a variety of improvements. The coolers could be controlled by programmable microcontrollers to eliminate the need for the control board and PC interface. High efficiency or multiple stage thermoelectric coolers could be used to increase effectiveness of interface heat transfer. Collaboration with

plastic manufacturers could produce more advanced gel pad materials with even higher thermal conductivities. Alternative heat sinks, such as thermoconductive plastics, fluid cooled bladders, or phase change materials could be used to reduce the overall weight and eliminate the need for the aluminum heat sink and cooling fan. Air loss (as described in 4.4.2) could be minimized by molding the space for the cushioning gel pad and sealing it within the cushion frame design

Third, an improved sensor array might be capable of gathering a more complete picture of the locally cooled area using a cushion with embedded cooling elements. Wireless skin-mounted sensors or thermistor-equipped undergarments could be implemented to more accurately control the TEC units by providing feedback directly to areas at risk for PU development. Thermal imaging methods are another option to record both interface and skin temperatures for the evaluation of future cool cushion designs.

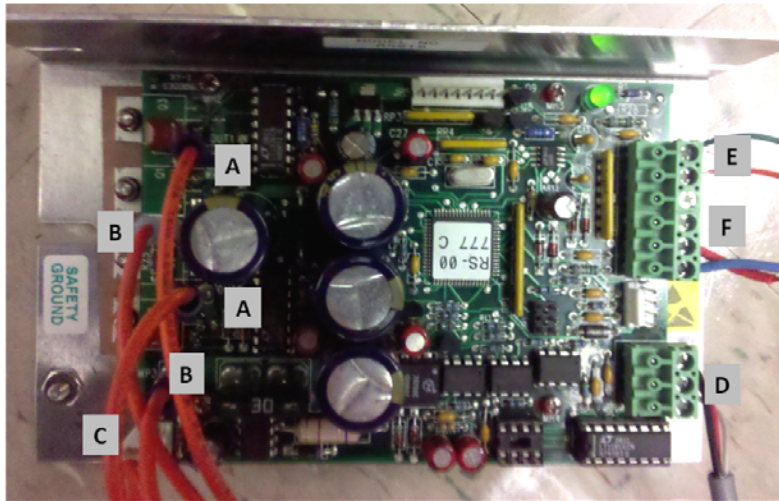
4.7 SUMMARY AND CONCLUSIONS

The results of this study showed that a closed loop controlled, site-specific cushion could effectively deliver local cooling in the desired protective range near 25°C. Skin temperatures normally increase over time on any standard cushion. Using our system, interface temperatures were not significantly different from the target after 15 min of seated use in all test sessions. Lower interface temperatures could reduce metabolic demand of ischemic tissue, decrease the severity of reperfusion injury, and increase the overall tissue tolerance for pressures in areas most at risk for pressure ulcer formation, specifically those of the IT regions. Introduction of thermoelectric cooling elements did not increase interface pressure, an indication that the

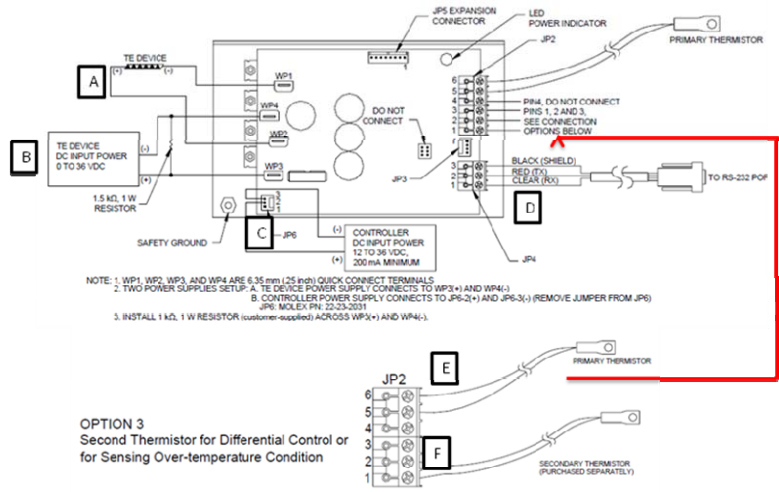
modified cushion would be an efficacious choice for both the redistribution of interface pressures and reduction of local temperatures. In a simulated trial using the TRCLI, our system was able to sustain a rate of local cooling when given a constant heat source for 3 hour duration. These trials did not meet the ideal protective temperature level of 25°C, but local cooling provided significantly reduced interface temperatures compared to the contralateral, uncooled IT. Further investigations into the effects of imbedded coolers on water vapor transmission characteristics must be conducted to better characterize the relationship between applied cooling and relative humidity at the interface. Our system illustrated a simple and effective means to deliver targeted local cooling which responds to changes in microenvironment.

APPENDIX A

CONTROL BOARD WIRING DIAGRAM



Controller Wiring Diagram: Two Power Supplies Setup



BIBLIOGRAPHY

1. Arnold, M.C., *Pressure ulcer prevention and management: the current evidence for care*. AACN Clinical Issues, 2003. **14**(4): p. 411-28.
2. Lyder, C.H., *Pressure ulcer prevention and management*. JAMA, 2003. **289**(2): p. 223-6.
3. Schoonhoven, L., et al., *The prevalence and incidence of pressure ulcers in hospitalised patients in the Netherlands: a prospective inception cohort study*. International Journal of Nursing Studies, 2007. **44**(6): p. 927-35.
4. Pancorbo-Hidalgo, P.L., et al., *Risk assessment scales for pressure ulcer prevention: a systematic review*. Journal of Advanced Nursing, 2006. **54**(1): p. 94-110.
5. Stewart, S. and J.S. Box-Panksepp, *Preventing hospital-acquired pressure ulcers: a point prevalence study*. Ostomy Wound Management, 2004. **50**(3): p. 46-51.
6. Beitz, J.M., *Overcoming barriers to quality wound care: a systems perspective*. Ostomy Wound Management, 2001. **47**(3): p. 56-64.
7. Chauhan, V.S., et al., *The prevalence of pressure ulcers in hospitalised patients in a university hospital in India*. Journal of Wound Care, 2005. **14**(1): p. 36-7.
8. Chicano, S.G. and C. Drolshagen, *Reducing hospital-acquired pressure ulcers*. Journal of Wound, Ostomy, & Continence Nursing, 2009. **36**(1): p. 45-50.
9. Reger, S.I., V.K. Ranganathan, and V. Sahgal, *Support surface interface pressure, microenvironment, and the prevalence of pressure ulcers: an analysis of the literature*. Ostomy Wound Manage, 2007. **53**(10): p. 50-8.
10. Russo, C.A. and A. Elixhauser, *Hospitalizations related to pressure sores, 2003*. Healthcare Cost and Utilization Project. Agency for Healthcare Research and Quality. Statistical Brief, 2006. **3**.

11. Kuffler, D.P., *Techniques for Wound Healing with a Focus on Pressure Ulcers Elimination*. 2010.
12. Kosiak, M., *Etiology of decubitus ulcers*. Archives of physical medicine and rehabilitation, 1961. **42**: p. 19.
13. Daniel, R.K., D.L. Priest, and D.C. Wheatley, *Etiologic factors in pressure sores: an experimental model*. Archives of physical medicine and rehabilitation, 1981. **62**(10): p. 492.
14. *National Pressure Ulcer Advisory Panel - support surface standards initiative terms and definitions*. Terms and definitions related to support surfaces 2007; Available from: www.npuap.org/NPUAP_S3I_TD.pdf.
15. Saito, Y., et al., *The loss of MCP-1 attenuates cutaneous ischemia–reperfusion injury in a mouse model of pressure ulcer*. Journal of Investigative Dermatology, 2008. **128**(7): p. 1838-1851.
16. Bouten, C.V., et al., *The etiology of pressure ulcers: skin deep or muscle bound?* Archives of physical medicine and rehabilitation, 2003. **84**(4): p. 616-619.
17. Bansal, C., et al., *Decubitus ulcers: a review of the literature*. International journal of dermatology, 2005. **44**(10): p. 805-810.
18. Linder-Ganz, E., et al., *Pressure-time cell death threshold for albino rat skeletal muscles as related to pressure sore biomechanics*. J Biomech, 2006. **39**(14): p. 2725–2732.
19. Brienza, D.M. and M.J. Geyer, *Using support surfaces to manage tissue integrity*. Advances in Skin & Wound Care, 2005. **18**(3): p. 151-7.
20. Tzen, Y.-T., *Effects of Local Cooling on Skin Perfusion response to Pressure: Implications to pressure Ulcer Prevention*, in *School of Health and Rehabilitation Sciences*. 2008, University of Pittsburgh: Pittsburgh, PA.
21. Tzen, Y.-T., *Effectiveness of local cooling on enhancing tissue ischemia tolerance in people with spinal cord injury*, in *School of Health and Rehabilitation Sciences*. 2010, University of Pittsburgh: Pittsburgh, PA.
22. Iaizzo, P.A., S. Quasthoff, and F. Lehmann-Horn, *Differential diagnosis of periodic paralysis aided by in vitro myography*. Neuromuscular Disorders, 1995. **5**(2): p. 115-24.

23. Kokate, J.Y., et al., *Temperature-modulated pressure ulcers: a porcine model*. Archives of Physical Medicine & Rehabilitation, 1995. **76**(7): p. 666-73.
24. Patel, S., et al., *Temperature effects on surface pressure-induced changes in rat skin perfusion: implications in pressure ulcer development*. J Rehabil Res Dev, 1999. **36**(3): p. 189-201.
25. Brienza, D., et al., *A Randomized Clinical Trial on Preventing Pressure Ulcers with Wheelchair Seat Cushions*. Journal of the American Geriatrics Society, 2010.
26. Brienza, D.M., et al., *The Relationship Between Pressure Ulcer Incidence and Buttock-Seat Cushion Interface Pressure in At-Risk Elderly Wheelchair Users**. Archives of physical medicine and rehabilitation, 2001. **82**(4): p. 529-533.
27. Brienza, D.M. and M.J. Geyer, *Using support surfaces to manage tissue integrity*. Advances in Skin & Wound Care, 2005. **18**(3): p. 151.
28. Eggert, R.J., *Engineering design*. 2005: Pearson Prentice Hall.
29. Black, J., et al., *National Pressure Ulcer Advisory Panel's updated pressure ulcer staging system*. Urologic Nursing, 2007. **27**(2): p. 144-50.
30. Ducker, A., *Pressure ulcers: assessment, prevention, and compliance*. Case Manager, 2002. **13**(4): p. 61-4; quiz 65.
31. Singh, R., et al., *Health-related problems and effect of specific interventions in spinal cord injury. An outcome study in Northern India*. European journal of physical & rehabilitation medicine., 2010. **46**(1): p. 47-53.
32. Statistics, N.C.f.H. *Multiple Cause of Death*. 1999-2001 [cited 2010].
33. Redelings, M.D., N.E. Lee, and F. Sorvillo, *Pressure ulcers: more lethal than we thought?* Advances in Skin & Wound Care, 2005. **18**(7): p. 367-72.
34. Gordon, M.D., et al., *Review of evidenced-based practice for the prevention of pressure sores in burn patients*. Journal of Burn Care & Rehabilitation, 2004. **25**(5): p. 388-410.
35. Kuhn, B.A. and S.J. Coulter, *Balancing the pressure ulcer cost and quality equation*. Nursing Economics, 1992. **10**(5): p. 353-9.

36. Jay, R., *Pressure and shear: their effects on support surface choice*. Ostomy/wound management, 1995. **41**(8): p. 36.
37. Levine, J., M.D. *How CMS Views Pressure Ulcers in Hospitals*. 2010 [cited 2010 June 17]; Available from: <http://jeffreylevinemd.com/cms-view-on-pressure-ulcers-in-hospitals/>.
38. Keller, P.B., et al., *Pressure ulcers in intensive care patients: a review of risks and prevention*. Intensive care medicine, 2002. **28**(10): p. 1379-1388.
39. Yarkony, G.M., *Pressure ulcers: a review*. Archives of physical medicine and rehabilitation, 1994. **75**(8): p. 908.
40. Landis, E.M., *Micro-injection studies of capillary blood pressure in human skin*. Heart, 1930. **15**(15): p. 209-228.
41. Reswick, J. and J. Rogers, *Experience at Rancho Los Amigos Hospital with devices and techniques to prevent pressure sores*. Bedsore biomechanics, 1976: p. 301–310.
42. Stekelenburg, A., et al., *Deep tissue injury: how deep is our understanding?* Archives of physical medicine and rehabilitation, 2008. **89**(7): p. 1410-1413.
43. Reddy, M., S. Gill, and P. Rochon, *Preventing pressure ulcers: a systematic review*. JAMA, 2006. **296**(8): p. 974.
44. Bergstrom, N., et al., *The Braden scale for predicting pressure sore risk*. Nursing Research, 1987. **36**(4): p. 205.
45. Jan, Y.K. and D.M. Brienza, *Technology for pressure ulcer prevention*. Topics in Spinal Cord Injury Rehabilitation, 2006. **11**(4): p. 30-41.
46. Goldstein, B. and J. Sanders, *Skin response to repetitive mechanical stress: a new experimental model in pig*. Archives of physical medicine and rehabilitation, 1998. **79**(3): p. 265-272.
47. Dinsdale, S., *Decubitus ulcers: role of pressure and friction in causation*. Archives of physical medicine and rehabilitation, 1974. **55**(4): p. 147.
48. Bennett, L., et al., *Shear vs pressure as causative factors in skin blood flow occlusion*. Archives of physical medicine and rehabilitation, 1979. **60**(7): p. 309.

49. Reddy, N.P., G.V.B. Cochran, and T.A. Krouskop, *Interstitial fluid flow as a factor in decubitus ulcer formation*. Journal of Biomechanics, 1981. **14**(12): p. 879-881.
50. Peirce, S.M., T.C. Skalak, and G.T. Rodeheaver, *Ischemia reperfusion injury in chronic pressure ulcer formation: A skin model in the rat*. Wound Repair and Regeneration, 2000. **8**(1): p. 68-76.
51. Arrhenius, S., *On the rate of reaction of the inversion of sucrose by acids*. Zeitschrift fuer physikalische Chemie, 1889. **4**: p. 226-48.
52. Brown AC, B.G., *Energy Metabolism*. Physiology and Biophysics, ed. P. HD. 1965, Philadelphia: Saunders.
53. Salcido, R., et al., *Histopathology of pressure ulcers as a result of sequential computer-controlled pressure sessions in a fuzzy rat model*. Advances in Skin & Wound Care, 1994. **7**(5): p. 23.
54. Patel, S., et al., *Temperature effects on surface pressure-induced changes in rat skin perfusion: implications in pressure ulcer development*. Development, 1999. **36**(3).
55. Fisher, S.V., et al., *Wheelchair cushion effect on skin temperature*. Arch Phys Med Rehabil, 1978. **59**(2): p. 68-72.
56. Van Beaumont, W. and R.W. Bullard, *Sweating: direct influence of skin temperature*. Science, 1965. **147**: p. 1465-1467.
57. Zimmerer, R., K. Lawson, and C. Calvert, *The effects of wearing diapers on skin*. Pediatric Dermatology, 1986. **3**(2): p. 95-101.
58. Ferguson-Pell, M., et al., *Thermodynamic rigid cushion loading indenter: A Buttock-shaped temperature and humidity measurement system for cushioning surfaces under anatomical compression conditions*. Journal of Rehabilitation Research & Design, 2009. **46**(7): p. 945-956.
59. Kokate, J.Y., et al., *Temperature-modulated pressure ulcers: a porcine model*. Arch Phys Med Rehabil, 1995. **76**(7): p. 666-73.
60. Iaizzo, *Prevention of pressure ulcers by focal cooling: Histological assessment in a porcine model*. Wounds (King of Prussia, Pa.), 1995. **7**(5): p. 161.

61. Harman, J.W., *The significance of local vascular phenomena in the production of ischemic necrosis in skeletal muscle*. The American Journal of Pathology, 1948. **24**(3): p. 625.
62. Lachenbruch, C., *Skin cooling surfaces: estimating the importance of limiting skin temperature*. Ostomy Wound Manage, 2005. **51**(2): p. 70-9.
63. Meijer, J., et al., *Method for the measurement of susceptibility to decubitus ulcer formation*. Medical and Biological Engineering and Computing, 1989. **27**(5): p. 502-506.
64. Mahanty, S. and R. Roemer, *Thermal response of skin to application of localized pressure*. Archives of physical medicine and rehabilitation, 1979. **60**(12): p. 584.
65. Mahanty, S. and R. Roemer, *Thermal and circulatory response of tissue to localized pressure application: a mathematical model*. Archives of physical medicine and rehabilitation, 1980. **61**(8): p. 335.
66. van Marum, R.J., J.H. Meijer, and M.W. Ribbe, *The relationship between pressure ulcers and skin blood flow response after a local cold provocation*. Arch Phys Med Rehabil, 2002. **83**(1): p. 40-3.
67. Liu, M.H., et al., *Transcutaneous oxygen tension in subjects with paraplegia with and without pressure ulcers: a preliminary report*. Age (years). **56**(6.00): p. 52-5.78.
68. Sae-Sia, W., D.D. Wipke-Tevis, and D.A. Williams, *The effect of clinically relevant pressure duration on sacral skin blood flow and temperature in patients after acute spinal cord injury*. Archives of physical medicine and rehabilitation, 2007. **88**(12): p. 1673-1680.
69. Sprigle, S., L. Press, and K. Davis, *Development of uniform terminology and procedures to describe wheelchair cushion characteristics*. J Rehabil Res Dev, 2001. **38**(4): p. 449-61.
70. Baranoski, S., E.A. Ayello, and I. Ovid Technologies, *Wound care essentials: Practice principles*. 2008: Lippincott Williams & Wilkins.
71. *The Roho Group - Cushion Adjustment Instructions*. 2003; Available from: <http://www.therohogroup.com/products/seat%20cushions/properadjust/instruction.html>.
72. Gilsdorf, P., et al., *Sitting forces and wheelchair mechanics*. Journal of rehabilitation research and development, 1990. **27**(3): p. 239.

73. Goossens, R.H., *Shear stress measured on three different materials*. LiquiCell Technologies, Inc, 2001.
74. Akins, J., P. Karg, and D. Brienza, *Interface shear and pressure characteristics of wheelchair seat cushions*. Journal of rehabilitation research and development, 2011. **48**(3).
75. Stewart, S.F., V. Palmieri, and G.V. Cochran, *Wheelchair cushion effect on skin temperature, heat flux, and relative humidity*. Arch Phys Med Rehabil, 1980. **61**(5): p. 229-33.
76. Brattgard, S., S. Carlsoo, and K. Severinsson. *Temperature and humidity in the sitting area*. 1976: University Park Press.
77. Plattner, O., et al., *Efficacy of intraoperative cooling methods*. Anesthesiology, 1997. **87**(5): p. 1089.
78. Knoll, T., et al., *The Low Normothermia Concept-Maintaining a Core Body Temperature Between 36 and 37 [degrees] C in Acute Stroke Unit Patients*. Journal of Neurosurgical Anesthesiology, 2002. **14**(4): p. 304.
79. Holzer, M., *Devices for rapid induction of hypothermia*. European Journal of Anaesthesiology, 2008. **25**(S42): p. 31-38.
80. Seder, D.B. and S. Jarrah, *Therapeutic hypothermia for cardiac arrest: A practical approach*. Current treatment options in neurology, 2009. **11**(2): p. 137-149.
81. Bernard, S., et al., *Induced hypothermia using large volume, ice-cold intravenous fluid in comatose survivors of out-of-hospital cardiac arrest::: a preliminary report*. Resuscitation, 2003. **56**(1): p. 9-13.
82. Felberg, R., et al., *Hypothermia after cardiac arrest: feasibility and safety of an external cooling protocol*. Circulation, 2001. **104**(15): p. 1799.
83. Janata, A., et al., *Therapeutic hypothermia with a novel surface cooling device improves neurologic outcome after prolonged cardiac arrest in swine**. Critical care medicine, 2008. **36**(3): p. 895.
84. Uray, T., et al., *Surface Cooling With a Novel Cooling-Blanket for Rapid Induction of Mild Hypothermia in Humans After Cardiac Arrest. A Feasibility Trial*.

85. Bayegan, K., et al., *Rapid non-invasive external cooling to induce mild therapeutic hypothermia in adult human-sized swine*. Resuscitation, 2008. **76**(2): p. 291-298.
86. Epstein, Y., Y. Shapiro, and S. Brill, *Comparison between different auxiliary cooling devices in a severe hot/dry climate*. Ergonomics, 1986. **29**(1): p. 41-48.
87. Givoni, B. and R.F. Goldman, *Predicting rectal temperature response to work, environment, and clothing*. Journal of Applied Physiology, 1972. **32**(6): p. 812.
88. Xu, X., et al., *Efficiency of liquid cooling garments: prediction and manikin measurement*. Aviation, space, and environmental medicine, 2006. **77**(6): p. 644-648.
89. Jetté, F.X., et al., *Effect of thermal manikin surface temperature on the performance of personal cooling systems*. European Journal of Applied Physiology, 2004. **92**(6): p. 669-672.
90. Lopez, R.M., et al., *Thermoregulatory influence of a cooling vest on hyperthermic athletes*. Journal of athletic training, 2008. **43**(1): p. 55.
91. O'Hara, R., et al., *Current and Future Cooling Technologies Used in Preventing Heat Illness and Improving Work Capacity for Battlefield Soldiers-Review of the Literature*. Military medicine, 2008. **173**(7): p. 653-657.
92. CHOI, J.W., M.J. KIM, and J.Y. LEE, *Alleviation of Heat Strain by Cooling Different Body Areas during Red Pepper Harvest Work at WBGT 33*. Industrial Health, 2008. **46**(6): p. 620-628.
93. Hamilton, A. and J. Hu, *An electronic cryoprobe for cryosurgery using heat pipes and thermoelectric coolers: a preliminary report*. Journal of medical engineering & technology, 1993. **17**(3): p. 104-109.
94. Holman, M.R. and S.J. Rowland, *Design and development of a new cryosurgical instrument utilizing the Peltier thermoelectric effect*. J Med Eng Technol, 1997. **21**(3-4): p. 106-10.
95. *HCPCS General Information*. April 1, 2011]; Available from: <http://www.cms.gov/MedHCPCSGenInfo/>.
96. Brienza, D.M., et al., *The relationship between pressure ulcer incidence and buttock-seat cushion interface pressure in at-risk elderly wheelchair users*. Archives of Physical Medicine & Rehabilitation, 2001. **82**(4): p. 529-33.

97. Sprigle, S. and M. Eicholtz. *Temperature and Humidity at the Buttock-Wheelchair Cushion Interface*. in *BMES Annual Meeting*. 2009. Pittsburgh, PA.
98. Sprigle, S., *The Science of Interface Pressure Mapping—Updates for Clinical Application*.
99. Sprigle, S., W. Dunlop, and L. Press, *Reliability of bench tests of interface pressure*. *Assistive technology: the official journal of RESNA*, 2003. **15**(1): p. 49.
100. Consulting, A.S., *The Effect of Temperature on Skin Ulcer Development*.
101. ISO, *CD 16840-7 Wheelchair seating, in The determination of heat and water vapour dissipation characteristics of seat cushions intended to manage tissue integrity*. 2003, International Organization for Standardization: Geneva, Switzerland.
102. Ferguson-Pell, M., et al., *Measurement of physical parameters at the patient-support interface*. Whittle M, Harris D [edsj. *Biomechanical measurement in orthopaedic practice*. Oxford: Clarendon Press, 1985: 133-44.
103. Judy, D., et al., *Improving the Detection of Pressure Ulcers Using the TMI ImageMed System*. *Advances in Skin & Wound Care*, 2011. **24**(1): p. 18.
104. Sprigle, S., et al., *Clinical skin temperature measurement to predict incipient pressure ulcers*. *Advances in Skin & Wound Care*, 2001. **14**(3): p. 133.
105. Garber, S.L. and T.A. Krouskop, *Wheelchair cushion modification and its effect on pressure*. *Arch Phys Med Rehabil*, 1984. **65**(10): p. 579-83.
106. PDAC, *HCPCS Code E2624 Product Search Results, in Medicare Pricing, Data Analysis, and Coding*. 2011, Noridian Administrative Services LLC.
107. Stinson, M., A. Porter-Armstrong, and P. Eakin, *Pressure mapping systems: reliability of pressure map interpretation*. *Clinical rehabilitation*, 2003. **17**(5): p. 504.
108. Hamanami, K., A. Tokuhira, and H. Inoue, *Finding the optimal setting of inflated air pressure for a multi-cell air cushion for wheelchair patients with spinal cord injury*. *Acta Medica Okayama*, 2004. **58**(1): p. 37-44.
109. Sprigle, S., et al., *Wheelchair Cushion Performance In Everyday use and How Wheelchairs are Used in Everyday Life*. 25th Annual Seating Symposium, 2009.

110. Cabanac, M., *Temperature regulation*. Annual review of physiology, 1975. **37**(1): p. 415-439.
111. Bullard, R., et al., *Skin temperature and thermoregulatory sweating: a control systems approach*. Physiological and Behavioral Temperature Regulation. Springfield, Mass.: Warren Porter Publications, 1970: p. 597–610.
112. Arkin, H., L. Xu, and K. Holmes, *Recent developments in modeling heat transfer in blood perfused tissues*. Biomedical Engineering, IEEE Transactions on, 1994. **41**(2): p. 97-107.
113. Oberg, B., et al., *Classical Thermodynamics of Wheelchair Cushions and Otto Bock ComforT Temperature Intervention*. The journal of the Utah Academy of Sciences, Arts, and Letters, 2003: p. 72.
114. Zhang, X., et al., *Measurements of the Thermal Conductivity and Thermal Diffusivity of Polymer Melts with the Short-Hot-Wire Method*. International Journal of Thermophysics, 2002. **23**(4): p. 1077-1090.